Trifluoromethyl sulphur pentafluoride, SF5CF3: atmospheric chemistry and its environmental importance via the greenhouse effect

Tuckett, Richard; Tressaud, A

DOI:
10.1016/S1872-0358(06)01003-7

Trifluoromethyl sulphur pentafluoride, SF_5CF_3 : atmospheric chemistry and its environmental importance *via* the greenhouse effect

R.P. Tuckett *

Advances in Fluorine Science (2006) **1**, chapter 3 (pp. 89-129) (Elsevier, ISBN 0-444-52811-3)
Fluorine and the Environment : atmospheric chemistry, emissions and lithosphere

DOI: 10.1016/S1872-0358(06)01003-7

Professor Richard Tuckett (University of Birmingham) / July 2011

(*v2 after comments of referee, 16.12.05*)

Trifluoromethyl sulphur pentafluoride, SF_5CF_3 : atmospheric chemistry and its environmental importance *via* the greenhouse effect

Richard P. Tuckett

School of Chemistry, University of Birmingham, Edgbaston, Birmingham, B15 2TT, U.K.

Number of pages : 31 (including references, but excluding table captions, tables, figure captions and figures)
Number of tables : 6
Number of figures : 13

Number of words : 16,250 (including references, tables, and figure captions)

Details for correspondence : tel : +44 121 414 4425, fax : +44 121 414 4403, email : r.p.tuckett@bham.ac.uk

---

Abstract One molecule of SF_5CF_3, an adduct of the SF_5 and CF_3 free radicals, causes more global warming than one molecule of any other greenhouse gas yet detected in the atmosphere, *i.e.* it has the highest *per molecule* radiative forcing of any greenhouse pollutant, and the value of its global warming potential is only exceeded by that of SF_6. Using tunable vacuum-UV radiation from a synchrotron and coincidence spectroscopy, the strength of the central S–C bond in SF_5CF_3 is determined to be 3.86 ± 0.45 eV or 372 ± 43 kJ mol^{-1}, and this molecule is very unlikely to be removed from the earth's atmosphere by UV photolysis in the stratosphere. Complementary laboratory-based experiments have shown that the main sink route of this greenhouse gas is low-energy electron attachment in the mesosphere, with Lyman-α photodissociation at 121.6 nm being only a minor channel. By comparison with data for SF_6, the lifetime of SF_5CF_3 in the earth's atmosphere is estimated to be *ca.* 1000 years. The principal reason for the current low level of concern about the impact of SF_5CF_3 on our environment is that the concentration levels are still very low, at the sub parts per trilllion level. The high growth rate of *ca.* 6% per annum, however, should cause concern for policymakers.

Keywords **:** SF_5CF_3, greenhouse gas, atmospheric lifetime, synchrotron radiation, photoionisation, TPEPICO, mesospheric reactions, ion-molecule, electron attachment, Lyman-α radiation

1. *Introduction*

Trifluoromethyl sulphur pentafluoride, SF_5CF_3, has recently been termed the super greenhouse gas. This claim to fame arises because, *per molecule*, it makes more contribution to global warming *via* the greenhouse effect than any other molecule yet detected in the atmosphere. Within this headline phrase, however, caution must be exercised because the amounts of SF_5CF_3 in the earth's atmosphere are still very low at the sub parts per trillion level by volume, *ca.* 0.15 pptv ; 1 pptv is equivalent to a number density of 2.46×10^7 molecules cm^{-3} for a pressure of 1 bar and a temperature of 298 K. By contrast, carbon dioxide has a current concentration in the earth's atmosphere of *ca.* 370 parts per million by volume, over nine orders of magnitude greater than that of SF_5CF_3. Despite a much lower environmental impact *per molecule*, CO_2 makes a much greater impact to global warming, simply because its concentration is much higher. Nevertheless, the Kyoto protocol of 1997, now ratified as an International Treaty in 2005, to limit emissions of greenhouse gases has meant that scientists and industry are now legally bound to determine the most environmentally-benign and cost-effective materials in large-scale industrial applications. It is therefore essential to understand the reactive and photochemical properties of molecules used in industry that are emitted into the atmosphere, even gases that at first sight might seem benign and harmless. It is within this near-worldwide political consensus for control of global warming that one can understand the huge upsurge in interest in SF_5CF_3 since its potential for global warming was first raised by Sturges *et al.* [1] five years ago.

SF_5CF_3 is a gas at room temperature, with a boiling point of 253 K and an enthalpy of vapourisation of 20.2 kJ mol^{-1} over the temperature range 223–253 K [2], and such thermochemical data has been available for some time. The paper by Sturges *et al.* [1], however, was the first to describe detection of SF_5CF_3 in the earth's atmosphere. Its source was believed to be anthropogenic in nature, and most likely a breakdown product of SF_6 in high-voltage equipment. Since the trends in concentration levels of SF_6 and SF_5CF_3 have tracked each other very closely over the last 30-40 years, Sturges *et al.* suggested that SF_5CF_3 has mainly been produced in the electronics industry *via* the recombination of SF_5 and CF_3 free radicals. This claim has since been disputed [3]. Infrared (IR) absorption measurements showed that SF_5CF_3 has the highest radiative forcing per molecule of any gas found in the atmosphere to date (0.57 W m^{-2} ppb^{-1}, a figure since updated to 0.60 ± 0.03 W m^{-2} ppb^{-1} [4,5]). Antarctic firn measurements suggested that it has grown from a concentration of near zero in the late 1960s to *ca*. 0.12 pptv in 1999 with a current growth rate of *ca.* 6% per annum, and stratospheric profiles suggested that the lifetime of this species in the atmosphere is between several hundred and a few thousand years. It was estimated that the global warming potential (GWP) of SF_5CF_3 is 18,000 relative to CO_2, with only SF_6 having a higher value. Sturges *et al.* concluded that, whilst still a relatively minor problem, nevertheless it was important to control the source(s) of SF_5CF_3 into the atmosphere in order to guard against an undesirable accumulation of this potent greenhouse gas. These comments remain as true now as they were then.

Furthermore, in historical terms, the story of the chlorofluorocarbons, and their 'conversion' from industrially-produced benign molecules to serious ozone-depleting molecules in the stratosphere over a period of less than 20 years, is still fresh in the memory of many atmospheric scientists. Small problems have a tendancy to become big problems in atmospheric science. Thus, although the best estimate two years ago was that SF_5CF_3 only contributes 0.003 % to the total greenhouse effect [6], it is not surprising that there has been huge interest in the reactive and photochemical properties of SF_5CF_3.

The purpose of this chapter is to review the microscopic properties of SF_5CF_3, most of them measurements and calculations made since Sturges *et al.* published their paper. Emphasis will be on those measurements that pertain to the atmospheric properties of SF_5CF_3 and the processes that remove it from the earth's atmosphere. Only limited descriptions of the macroscopic properties of SF_5CF_3 will be given. Since the readership of this chapter will be wide, the terms *microscopic* and *macroscopic* may mean different things to different readers. As a chemical physicist, I define a microscopic property to be that of one molecule of the system under study (*e.g.* a spectroscopic, kinetic, photochemical or thermodynamic property). A macroscopic property relates to the system as a whole (*e.g.* industrial production sources of SF_5CF_3, the geographical properties that determine the transport of SF_5CF_3 through the atmosphere *via* convection and diffusion). The chapter will conclude with a review of the properties of SF_5CF_3 that determine its lifetime in the earth's atmosphere. The *lifetime* of a pollutant is another term that can mean different things to different scientists, and I will bring together all the many interpretations of this term in the context of the physical, chemical and geographical properties of SF_5CF_3 in our atmosphere.

2. *Structure, spectroscopy and thermochemistry of SF_5CF_3*

It is of some surprise to note that SF_5CF_3 is not a new molecule, and its microwave spectrum was recorded by Kisliuk and Silvey [7] as long ago as 1952. The S–C bond distance was determined to be 0.186 nm, and in 1985 all the geometrical parameters for SF_5CF_3 were reported by Marsden *et al.* [8] from an electron diffraction study. Figure 1 shows an unpublished structure of the highest occupied molecular orbital (HOMO) of SF_5CF_3 by Knowles [9] using the MOLPRO *ab initio* suite of programmes. The particular points to note are the substantial dipole moment of the molecule, 0.95 Debye, the significant σ-bonding electron density along the S–C bond, the S-C bond length of 0.187 nm in almost exact agreement with the microwave study, and the FSF and FCF bond angles of approximately 90^o or 109.3^o, respectively. SF_5CF_3 can therefore either be regarded as a perturbed SF_6 molecule in which one fluorine atom has been replaced by a CF_3 group of tetrahedral symmetry, or as a perturbed CF_4 molecule in which one fluorine has been replaced by an SF_5 group with octahedral symmetry. This will form a recurring theme of this chapter. The only major difference from SF_6 and CF_4 is that the HOMO of these two

molecules is a F 2pπ non-bonding in character, whereas the HOMO of SF_5CF_3 is S–C σ-bonding in character. The gas-phase IR and liquid-phase Raman spectra over the extended range of 100-4000 cm^{-1} were reported at low resolution over 40 years ago [10,11]. These measurements have been made at much higher resolution in the last three years, and all the important IR-active vibrations in the atmospheric window region of *ca*. 700-1500 cm^{-1} have been determined [12-14]. Of particular note is the determination by two groups of the integrated absorption coefficient over this range as a function of temperature between 200 and 300 K [13,14], both studies demonstrating that it showed little variation with temperature. There were no other spectroscopic details (*e.g.* UV/visible electronic, vacuum-UV photoionisation) on this molecule before the Sturges *et al.* [1] paper was published. Since 2000, there have been a large number of new studies, some of direct importance to the atmospheric properties of SF_5CF_3, some of more general and pure scientific interest. They include VUV and XUV absorption [4,15-19], valence photoelectron [4,15,20-22], electron energy loss spectroscopy [4,23], electron scattering [24-26], protonation [27] and photofragmentation studies [20-22,28].

As with the spectroscopic situation, there was scant information on the thermochemistry of SF_5CF_3 prior to 2000. The JANAF tables of 1998 [29] quote an enthalpy of formation of -1700 ± 63 kJ mol^{-1} at 0 K, -1717 ± 63 kJ mol^{-1} at 298 K, although these data are indirect and it is not clear how these numbers are derived. The strength of the SF_5–CF_3 σ-bond will also be determined by the enthalpies of formation of the SF_5 and CF_3 radicals, where improved values since the tables were published are now available. Since the strength of this bond is related to possible photochemistry of SF_5CF_3 that may occur in the stratosphere, a *direct* determination of $\Delta_f H^o$ (SF_5CF_3) is therefore essential to explain any possible atmospheric reactions. Such an experiment is described in Section 5.3. As with experimental spectroscopic studies, there have been many theoretical studies on SF_5CF_3 since 2000 [30-34]. Their main aim has been to determine properties that relate to the atmospheric chemistry of SF_5CF_3, such as integrated infrared intensities, vibrational frequencies, and thermochemical and structural parameters.

3. *The greenhouse effect and SF_5CF_3 : how serious is the problem ?*

The greenhouse effect is usually associated with small polyatomic molecules such as CO_2, H_2O, CH_4, N_2O and O_3. The 'natural' greenhouse gases, notably CO_2 and H_2O, have been responsible for hundreds of years for maintaining the temperature of the earth at *ca.* 290 K, suitable for habitation. The 'enhancing' greenhouse gases, mainly CH_4, N_2O and O_3, have concentrations in the atmosphere which have increased in the last 50-100 years, have IR absorptions in the atmospheric window region where CO_2 and H_2O do not absorb, and are believed to be the main culprits for global warming. It is now clear, however, that there are larger polyatomic gases of low concentrations in the atmosphere which can contribute significantly to global warming because they possess exceptionally strong IR absorption bands

in regions where other greenhouse gases do not absorb. Two notable examples are SF_6, which has a GWP of 22,200 relative to CO_2 over a time horizon of 100 years [35] and SF_5CF_3, the subject of this review. In qualitative terms, the physical and chemical properties that are necessary for a molecule to have a large GWP are : (a) it must absorb IR region in the black-body range of the earth's emission, *ca.* 5–25 μm (2000–400 cm^{-1}) with a peak at 15 μm (667 cm^{-1}) , in regions where CO_2 and H_2O do not absorb ; in practice this means many C–F and C–Cl stretching vibrations around 900-1100 cm^{-1} contribute strongly, (b) the integrated absorption intensities of the IR-active vibrations must be strong due to large dipole moment derivatives, (c) the molecule must have a long lifetime (defined in Section 7) in the earth's atmosphere ; it must not be photodissociated by solar UV radiation in either the troposphere ($\lambda > 290$ nm) or the stratosphere ($200 < \lambda < 290$ nm), and it must not react with either the OH or $O^*(^1D)$ free radicals. Furthermore, a greenhouse gas whose concentration is increasing rapidly due to man's activity, whilst not affecting directly an integrated absorption coefficient or the GWP value, is a special cause for concern for policymakers in Government.

SF_5CF_3 appears to obey all these criteria, and Table 1 shows data for five greenhouse gases which demonstrate how serious or otherwise the presence of SF_5CF_3 in the earth's atmosphere as a pollutant should be regarded. The five compounds are CO_2 and CH_4 which contribute *ca.* 70% to the overall greenhouse effect, N_2O, a chlorofluorocarbon, and SF_5CF_3. Most of the data is taken from the Intergovernmental Panel of Climate Change report of 2001 [35], an associated paper whose data fed into the IPCC2001 report [36], and one of many websites from an enviromental pressure group highlighting statistics on global warming [37]. Whilst some of the data may now be slightly out of date, the longterm trends should be unchanged. The term that is used to characterise the IR absorption properties of a greenhouse gas is the *radiative forcing*, whilst the overall effect of this pollutant on the earth's climate is described by the *global warming potential*. The former measures the strength of the absorption bands over the infrared black-body region of the earth, *ca.* 400-2000 cm^{-1}. Essentially, it is a (per molecule) microscopic property, is given the symbol a_o, and is usually expressed in units of W m^{-2} $ppbv^{-1}$. If this value is multiplied by the change in concentration of pollutant over a defined time window, usually the 250 years from before the Industrial Revolution to the current day, the macroscopic radiative forcing in units of W m^{-2} is obtained. One may then compare the radiative forcing of different pollutant molecules over this time window.

The GWP measures the radiative forcing, A_x, of a pulse emission of a greenhouse gas, x, over a defined time period, t, usually 100 years, relative to the time-integrated radiative forcing of a pulse emission of an equal mass of CO_2 [35] :

$$\mathrm{GWP}_x(t) \;=\; \frac{\int_0^t A_x(t).dt}{\int_0^t A_{CO2}(t).dt} \qquad \text{(I)}$$

The GWP is therefore a dimensionless number that informs how important one molecule of pollutant x is to the greenhouse effect *via* global warming compared to one molecule of CO_2. The GWP of CO_2 is defined to be unity. For most greenhouse gases, the radiative forcing following an emission at $t = 0$ takes a simple exponential form :

$$A_x(t) \;=\; A_{o,x}\exp(-t \,/\, \tau_x) \qquad \text{(II)}$$

where τ_x is the lifetime for removal of species x from the atmosphere. For CO_2, the lifetime ranges from 50 to 200 years [37,38], a single exponential decay is not appropriate, and we can write :

$$A_{\mathrm{CO2}}(t) \;=\; A_{\mathrm{o,CO2}}\left[\, b_o + \sum_{\mathrm{i}} b_i \exp(-t \,/\, \tau_{\mathrm{i}}) \right] \qquad \text{(III)}$$

where the response function, the bracket in the right-hand side of equ. (III), is derived from more complete carbon cycles. Values for b_i (i = 0-4) and τ_i (i = 1-4) have been given by Shine *et al.* [38]. It is important to note that the radiative forcing, A_o, in equs. (I)-(III) has units of W m^{-2} kg^{-1}. For this reason, it is given a different symbol to the microscopic radiative forcing, a_o, which has units of W m^{-2} ppbv^{-1}. Conversion between the two units is simple [38]. The time integral of the large bracket on the right-hand side of equ. (III), defined K_{CO2}, has units of time, and takes values of 13.44 and 45.73 years for a time period of 20 and 100 years, respectively, the values of t for which GWP values are most often quoted. Within the approximation that the greenhouse gas x follows a single-exponential time decay in the atmosphere, it is then possible to parameterise equ. (I) to give an exact analytical expression for the GWP of x over a time period t :

$$\frac{GWP_x(t)}{GWP_{CO2}(t)} \;=\; \frac{MW_{CO2}}{MW_x}.\frac{a_{o,x}}{a_{o,CO2}}.\frac{\tau_x}{K_{CO2}}.\left[1-\exp\left(\frac{-t}{\tau_x}\right)\right] \qquad \text{(IV)}$$

In this simple form, the GWP only incorporates values for the microscopic radiative forcing of greenhouse gases x and CO_2, $a_{o,x}$ and $a_{o,CO2}$, in units of W m^{-2} ppbv^{-1} ; the molecular weights of x and CO_2 ; the lifetime of x in the atmosphere, τ_x ; the time period over which the effect of the pollutant is determined ; and the constant K_{CO2} which can easily be determined for any value of t. This equation is not given in this specific form in [38], but is easy to derive from equations given therein. Note that a

similar equation given in Section 6 of reference [5] by Mason *et al.* has numerous typographical errors, and should be disregarded. The *recent* increase in concentration per unit time interval of a pollutant (*e.g.* the rise in concentration per annum over the last 5-10 years), one of the factors of most concern to policymakers, does not contribute directly to the GWP value. This and other factors [38] have caused some criticism of the use of GWPs in policy formulation. That said, the important point to note from Table 1 is that CO_2 and CH_4 contribute most to the greenhouse effect simply due to their high atmospheric concentration ; the radiative forcing per molecule and GWP of both gases are relatively low. By contrast, SF_5CF_3 has the highest radiative forcing per molecule of any greenhouse gas and its GWP value is therefore very high, but its contribution to the overall greenhouse effect is relatively small, because the concentration of SF_5CF_3 in the atmosphere is still very low.

4. *Kinetics and removal processes of SF_5CF_3 from the earth's atmosphere*

Even if the presence of SF_5CF_3 in our atmosphere contributes only a very small amount to global warming, nevertheless it is important to understand better the physical and chemical properties of this new greenhouse gas. It is especially important to determine what are the chemical and photolytic reactions that remove it from the atmosphere, since they will contribute to its lifetime and GWP value. The total rate of removal of SF_5CF_3 per unit volume per unit time is given by

$$\text{Rate} = [SF_5CF_3].\left(k_1[OH] + k_2[O^*(^1D)] + \sum_{ions} k_{ion}[ion] + k_e[e^-] + \sum_{\lambda} \sigma_\lambda J_\lambda \Phi_\lambda \right) \qquad \text{(V)}$$

where each of the five terms in the large bracket of equ. (V) is a pseudo-first-order rate constant. The first four terms represent reactions of SF_5CF_3 with OH, $O^*(^1D)$, cations and electrons, respectively ; k_1, k_2, k_{ion} and k_e are the corresponding second-order bimolecular rate coefficients. The first term will dominate in the troposphere (0 < altitude (h) < 10 km), the second term in the stratosphere (10 < h < 50 km), and the third and fourth terms in the mesosphere (h > 50 km). In the fifth term of the bracket, σ_λ and J_λ are the absorption cross section for SF_5CF_3 and the solar flux at wavelength λ, respectively, and Φ_λ is the quantum yield for dissociation following photoabsorption at wavelength λ. In the troposphere, the summation for λ is over the range *ca.* 290-700 nm, in the stratosphere *ca.* 200-290 nm, and in the mesosphere the solar flux at the Lyman-α wavelength of 121.6 nm dominates all other vacuum-UV wavelengths. We note that equation (V) assumes that the ion-molecule and electron attachment reactions lead to the removal of every SF_5CF_3 molecule by formation of dissociation products. Furthermore, secondary reactions of such products must not recycle SF_5CF_3. This assumption is true for ion-molecule reactions, but is not necessarily so for electron attachment (Section 6.2).

Having no hydrogen atoms, SF_5CF_3 is very unlikely to be removed by reaction with OH in the troposphere, and the rate coefficient for this reaction is almost certainly too small to measure by conventional laboratory techniques (*e.g.* discharge flow or pulsed photolysis with laser-induced fluorescence detection of OH). Likewise, the reaction of $O^*(^1D)$ with SF_5CF_3 has not been measured. There are therefore no chemical processes that remove SF_5CF_3 from the troposphere and stratosphere. Furthermore, the electron energy loss spectrum of SF_5CF_3, in effect a pseudo-absorption spectrum, showed that no bound excited electronic states exist for $h\nu <$ *ca.* 8 eV (*i.e.* $\lambda > 150$ nm) [23]. Therefore, σ_λ is effectively zero in both the relevant wavelength ranges of the troposphere and stratosphere. These laboratory measurements confirm field measurements reported by Sturges *et al.* [1] from stratospheric profiling that the lifetime of SF_5CF_3 in the earth's atmosphere is very long. In Section 5.2, an experiment is described to determine the strength of the $SF_5–CF_3$ bond, leading to an improved value for the enthalpy of formation of SF_5CF_3 [20,21]. This experiment was performed in the middle of 2000, the authors having obtained an early preprint of the Sturges paper. The principal concern of meterologists then was to determine this bond strength. The result, that the S–C bond has strong σ-character with a dissociation energy of *ca*. 4 eV or 400 kJ mol^{-1}, confirmed that UV photolysis in the stratosphere was very unlikely to contribute to the rate of removal of SF_5CF_3 from the atmosphere. In retrospect, and given experiments that have been performed since, this is an obvious result. Attention in recent years has therefore turned to laboratory-based measurements relevant to the mesosphere, where ionic processes involving cations, anions and electrons dominate, and where the only significant photolytic wavelength is 121.6 nm. These experiments are described in Section 6. In Section 7, I draw together all these data, and describe how the lifetime of SF_5CF_3, *ca.* 1000 years, is defined and determined.

5. *The VUV photoionisation and photofragmentation spectroscopy of SF_5CF_3*

5.1 *Definition of the first dissociative ionisation energy : application to CF_4 and SF_6*

Photodissociation generally occurs through excitation of a molecule to a repulsive electronic state which lies above a dissociation threshold. Close to threshold, the cross section for photodissociation can be negligibly small, and this makes the experimental determination of a dissociation energy notoriously difficult. Thus, CF_4 has a dissociation energy (to CF_3 + F) of 5.61 eV, but VUV photons with energies in excess of 12 eV are required to photodissociate CF_4. Likewise, the bond dissociation energy of SF_6 (to SF_5 + F) is 3.82 eV, but photodissociation is not observed until the photon energy exceeds *ca.* 10 eV. SF_5CF_3 seems to show similar properties. The electron energy loss spectrum [23] suggests that there are no excited electronic states of SF_5CF_3 lying less than *ca.* 8 eV above the ground state. In the stratosphere, the highest-energy solar photons have an energy of *ca.* 6 e (λ = *ca.* 200 nm). It is therefore very unlikely that SF_5CF_3 will be photodissociated in the stratosphere, irrespective of the strength of the S–C bond,

simply because dissociative electronic states at energies accessible with stratospheric UV photons are not present. The use of *neutral* excited states of SF_5CF_3 to determine its dissociation energy to $SF_5 + CF_3$ is therefore not viable.

CF_4, SF_6 and SF_5CF_3, however, also share the common property that the parent cation is not observed in a conventional 70 eV electron-impact mass spectrum [39]. Thus the ground electronic state of these cations is repulsive in the Franck-Condon region, dissociating on a time scale much faster than the transit time of an ion through a magnetic or quadrupole mass spectrometer. With CF_4 and SF_6, CF_3–F and SF_5–F bond cleavage to form CF_3^+ or $SF_5^+ + F + e^-$ must occur. With SF_5CF_3, we assume that cleavage of the central S–C bond occurs, forming either $SF_5^+ + CF_3 + e^-$ or $CF_3^+ + SF_5 + e^-$. Since the threshold energy of the latter dissociation channel lies *ca.* 0.8 eV lower than that of the former, we assume dissociation within the mass spectrometer to $CF_3^+ + SF_5 + e^-$ dominates. (We note that dissociation to $SF_4^+ + CF_4 + e^-$ requires even less energy [20,22], driven by the large and negative enthalpy of formation of CF_4, but the significant re-arrangement of chemical bonds needed in the transition state makes this reaction kinetically unfavourable.) Taking SF_5CF_3 as an example, we can define the first *dissociative ionisation energy* (DIE) of these molecules to be the 0 K energy of $CF_3^+ + SF_5 + e^-$ relative to the ground vibronic level of the neutral molecule (Figure 2). This energy has alternatively been called the adiabatic ionisation energy of the neutral molecule, but it is this author's belief that this latter terminology is inappropriate in cases such as CF_4, SF_6 and SF_5CF_3 where the Franck-Condon overlap at threshold is zero. The determination of the DIE of a molecule whose ground state of the parent ion is totally repulsive in the Franck-Condon region is a difficult problem, because its value is likely to be significantly less than the energy corresponding to the onset of ionisation of the neutral precursor ; in the opinion of this author, *onset of ionisation* is a more appropriate phrase to use than *adiabatic ionisation energy* for such molecules, since the latter term has ambiguous meanings. Thus the photoelectron spectrum of the parent molecule can only give an upper bound to its first DIE.

This problem is well known for CF_4 and SF_6, and for many years the DIE of these molecules has been the subject of controversy. However, Figure 2 can also apply to dissociation of a polyatomic molecule to two molecular free radicals. From the figure, it is clear that :

$$\text{DIE (ABCD)} = D_o(\text{AB–CD}) + \text{AIE (AB)} \qquad \text{(VI)}$$

where ABCD refers to a general polyatomic molecule which dissociates along the central B–C bond, D_o(AB–CD) is the dissociation energy of the AB–CD bond, and AIE (AB) is the adiabatic ionisation energy of the AB free radical ; in this situation, the use of *adiabatic ionisation energy* is appropriate so long as the ground state of AB^+ is bound in the Franck-Condon region. For SF_5CF_3, AB will clearly be

the CF_3, and CD the SF_5 radical. For SF_5CF_3, the estimation of its first DIE needs a knowledge of both the SF_5–CF_3 bond energy and the AIE of the CF_3 radical. The latter value is now well determined, 9.04 ± 0.04 eV [40], after many years of uncertainty, but when Sturges *et al.* [1] published their paper the former value was only known within a broad range of *ca.* 2-4 eV.

One method to determine the DIE of such molecules directly is to turn the problem around, and use the fact that, in the Franck-Condon region, the ground state of the parent cation lies above the DIE as a benefit rather than a hindrance. The fragments will be formed with translational kinetic energy, and we can perform a photoelectron – photoion coincidence (PEPICO) experiment to measure the mean translational kinetic energy, $\langle KE \rangle_T$, released into the AB^+ + CD fragments ; CD is atomic F for dissociation of CF_4 or SF_6. Using tunable vacuum-UV radiation, it is most convenient to use *threshold* photoelectron detection, and the acronym for this mode of spectroscopy then becomes TPEPICO. From an analysis of the width and shape of the fragment ion (AB^+) time-of-flight distribution in the TPEPICO spectrum measured at a photon energy hν, it is possible to determine $\langle KE \rangle_T$. This KE release will correspond to some fraction of the available energy, where

$$E_{avail} = h\nu + (\text{thermal energy of ABCD}) - \text{DIE(ABCD)} \qquad \text{(VII)}$$

The thermal energy of the parent neutral molecule comprises contributions from rotational energy ($3k_BT/2$ per molecule) and vibrational energy ($h\nu_i / exp(h\nu_i/k_BT)-1$, summed up for all vibrational modes ν_i). The size of this fraction, $\langle KE \rangle_T / E_{avail}$, is governed by the dynamics of the decay mechanism [41]. The mechanism cannot unambiguously be determined from a measurement at one single photon energy. By measuring $\langle KE \rangle_T$ continuously as a function of (hν + thermal energy of ABCD), however, and assuming that the fractional KE release is independent of energy, an extrapolation to a KE release of zero gives an intercept on the *x*-axis corresponding to the DIE of ABCD (Figure 3). As the AB^+–CD bond breaks, if dissociation involves an impulsive release of energy so great that it results in intramolecular collisions between the recoiling fragments (the 'pure' impulsive model), then $\langle KE \rangle_T$ and E_{avail} are related only by the kinematics of the dissociation [42] :

$$\langle KE \rangle_T = \frac{\mu_{B,C}}{\mu_{AB,CD}} . E_{avail} \qquad \text{(VIII)}$$

where $\mu_{B,C}$ is the reduced mass of the two atoms in the dissociating bond, and $\mu_{AB,CD}$ is the reduced mass of the two products of the dissociation. Thus the slope of the graph in Figure 3 is given simply by the ratio of two reduced masses. As a test of the experiment, we used this method to determine the first DIE

for CF_4 and SF_6, where there is now some degree of certainty in the correct values. From the former experiment, we determined the first DIE of CF_4 to be 14.45 ± 0.20 eV. Hence we were able to determine the 0 K enthalpy of formation of CF_3^+ to be 390 ± 20 kJ mol^{-1} and, *via* $\Delta_f H^o_0$ (CF_3) [40], the adiabatic ionisation energy of the CF_3 free radical. Our value, 8.84 ± 0.20 eV, was in good agreement with the now-accepted best experimental determination of 9.04 ± 0.04 eV [40]. The SF_6 experiment determined its first DIE to be 13.6 ± 0.1 eV, leading to a value for $\Delta_f H^o_0$ (SF_5^+) of 29 ± 10 kJ mol^{-1}. Using the recommended value for $\Delta_f H^o_0$ (SF_5) from the ion beam study of Fisher *et al.* [43], we obtained a value for the adiabatic ionisation energy of the SF_5 free radical of 9.8 ± 0.2 eV. Within error limits, this value is also in good agreement with the guided ion beam result of 9.60 ± 0.05 eV [43]. Following these test experiments, full details of which are given elsewhere [20,21], we measured the first DIE of SF_5CF_3 (Section 5.3). Using the now well-established ionisation energy of CF_3, we were able to determine, admittedly in an indirect manner, the dissociation energy of the SF_5–CF_3 bond.

5.2 *Experimental details*

The apparatus used for the TPEPICO study [44] is shown in Figure 4, the source of radiation being beamline 3.1 (1 m Seya-Namioka monochromator) of the UK Daresbury Synchrotron Radiation Source operating at a resolution of 0.3 nm. The monochromatised radiation is coupled into the interaction region *via* a capillary, and its flux is monitored from the fluorescence of a sodium salicylate coated window. Threshold photoelectrons and fragment cations from the interaction region are extracted in opposite directions by an electric field of 20 V cm^{-1}. The threshold electron analyser consists of a cylindrical electrostatic lens followed by a 127° post analyser, which rejects energetic electrons. The lens has a shallow depth of field and poor chromatic aberrations, so that only electrons with low initial energies produced in the centre of the interaction region focus efficiently at the entrance of the post analyser. Simulations suggest a high degree of space focusing, so a finite interaction volume is relatively unimportant. The resolution of the electron analyser, *ca.* 10 meV, is superior to that of the monochromator in these experiments, therefore the overall resolution of the experiment is limited by that of the photon source. Ions pass through a two-stage acceleration region followed by a linear time-of-flight (TOF) drift tube. This arrangement satisfies the space focusing condition, yielding sufficient TOF resolution that kinetic energy releases from dissociative ionisation events can be measured. Signals from the channeltron and microchannel plate detectors are discriminated and conveyed to a time-to-digital converter (TDC) card *via* pulse-shaping electronics. The electron signal provides the start pulse, the ion signal the stop pulse, and delayed coincidences can be recorded. Concurrently, the total ion yield and threshold photoelectron spectrum (TPES) can also be measured.

With this apparatus, three different spectra can be recorded. First, the TPES spectrum is obtained by recording the threshold electron signal as a function photon energy. Second, a TPEPICO spectrum is obtained by recording the coincidence spectrum continuously as a function of photon energy. The data record as a 3D map of coincidence counts *vs.* ion time of flight *vs.* photon energy. Sections from this map can yield either the time-of-flight mass spectrum at a defined photon energy or the yield of a particular ion. Third, with a fixed photon energy, high resolution TOF spectra can be recorded and values for $\langle KE \rangle_T$ obtained [45,46]. Briefly, for each TPEPICO-TOF spectrum a small basis set of peaks, each with a discrete energy release ε_t is computed, and assigned a probability. The discrete energies are given by $\varepsilon_t(n) = (2n-1)^2\Delta E$, where n = 1,2,3,4 ….. ΔE depends on the statistical quality of the data ; the higher the signal-to-noise ratio, the lower ΔE and the higher n can be set to obtain the best fit. Each computed peak in the kinetic energy release distribution spans the range $4(n-1)^2\Delta E$ to $4n^2\Delta E$, centred at $\varepsilon_t(n) + \Delta E$. The reduced probability of each discrete energy, $P(\varepsilon_t)$, is varied by linear regression to minimise the least-squared errors between the simulated and experimental TOF peak. From the basis set of ε_t and $P(\varepsilon_t)$, $\langle KE \rangle_T$ is easily determined.

5.3 *Determination of the first dissociative ionisation energy of SF_5CF_3 and the S–C bond strength*

The three modes of experiment described above were performed for SF_5CF_3 [20]. In addition, to determine the first DIE, important aspects of the second and third mode were combined. Thus the TOF spectrum for CF_3^+ was recorded over a narrow time window with a resolution of 16 ns, close to the optimum of the TDC card of 8 ns, and 64 wavelength channels were scanned over the energy range 12.9-15.7 eV, encompassing the Franck-Condon zone of the ground state of $SF_5CF_3^+$. The results are shown in Figure 5. Only those datapoints that define the Franck-Condon region, *ca.* 13.2-14.8 eV, were used to determine the slope and intercept of the graph. The onset of ionisation for SF_5CF_3, 12.9 ± 0.2 eV, lies significantly lower in energy than that in either CF_4 or SF_6, reflecting the different character of the HOMO. The mean KE releases over these channels range from 0.05 eV to 0.4 eV. As one example, Figure 6 shows the TPEPICO-TOF spectrum of CF_3^+/SF_5CF_3 recorded at 14.09 eV and the best simulated fit, from which a mean KE release of 0.24 ± 0.05 eV was determined. Within experimental error, the 35 lowest-energy data points which encompass the Franck-Condon region of the ground state of $SF_5CF_3^+$ fit to a straight line with a slope of 0.19, in excellent agreement with the prediction of the pure-impulsive model of 0.20. Extrapolation to a KE release of zero on the *y*-axis yields the first DIE of SF_5CF_3 to $CF_3^+ + SF_5 + e^-$ to be 12.9 ± 0.4 eV. The relatively large error in the DIE reflects the small slope of the $\langle KE \rangle_T$ *vs.* photon energy graph, and hence the shallow nature of the extrapolation. We should note that the DIE, unlike that of CF_4 and SF_6, is coincidentally isoenergetic with the ionisation onset of the first photoelectron band of SF_5CF_3 ; for CF_4 and SF_6, in both cases the first DIE lies over 1 eV lower than the onset of ionisation, leading to a longer extraoplation to zero $\langle KE \rangle_T$.

Two important thermochemical data can now be determined. First, using values for the 0 K enthalpies of formation of CF_3^+ (409 ± 3 kJ mol^{-1}) [40] and SF_5 (–915 ± 18 kJ mol^{-1}) [43], we determine $\Delta_f H^o_0$ (SF_5CF_3) to be –1750 ± 47 kJ mol^{-1}, significantly lower than that quoted in the 1998 JANAF tables [29]. Second, using the now-accepted value for AIE (CF_3) of 9.04 ± 0.04 eV [40], we determine the dissociation energy of the SF_5–CF_3 bond at 0 K to be 3.86 ± 0.45 eV or 372 ± 43 kJ mol^{-1}. (We note that these values are updates of those published in reference [20], following improvements in the published thermochemical values for CF_3 and CF_3^+.) Using the value for AIE (SF_5) with the highest claim for accuracy from Fisher *et al.* [43], 9.60 ± 0.05 eV, the *second* DIE of SF_5CF_3 (defined here to be $SF_5^+ + CF_3 + e^-$) is calculated to be 13.46 ± 0.45 eV. This energy is *ca.* 0.6 eV higher than the first DIE to $CF_3^+ + SF_5 + e^-$, and presumably explains why only CF_3^+ is observed for dissociation of the low-energy regions of the ground-state potential of $SF_5CF_3^+$.

At this stage it is only proper to highlight the assumptions and limitations of this extrapolation technique. The errors quoted for the first DIE of CF_4, SF_6 and SF_5CF_3 arise from random statistical errors in the data for $\langle KE \rangle_T$. Two factors have been ignored which might produce systematic errors. First, the theory assumes dissociation is 100% impulsive with no statistical component. The simple relation between $\langle KE \rangle_T$ and E_{avail} (equ. (VIII)) arises from classical mechanics, with linearity in the extrapolation graph (Figure 3) applying even for very low values of $\langle KE \rangle_T$. This is most likely to be true when the onset of ionisation to $ABCD^+$ is significantly greater than the DIE of ABCD, *i.e.* the situation for CF_4 and SF_6, but not perhaps for SF_5CF_3. Second, anisotropic effects are ignored in the analysis, despite the vacuum-UV radiation source being close to fully plane-polarised perpendicular to the time-of-flight axis. More details of these potential problems are given elsewhere [20].

Theoretical values for $\Delta_f H^o_0$ (SF_5CF_3) are significantly less negative than the experimental value, yielding weaker SF_5–CF_3 bond strengths. Ball [30] and Miller *et al.* [32], both using Gaussian-2 and Gaussian-3 Moller-Plesset perturbation methods, obtain $\Delta_f H^o_0$ to be –1615 and –1623 kJ mol^{-1}, respectively, the former being the average of G2 and G3 calculations. Using experimental values for the 0 K enthalpy of formation of CF_3 and SF_5 [40,43], they yield S–C bond strengths of 237 and 245 kJ mol^{-1}, respectively. It is worth noting that, whilst there has been convergence in recent years between experiment and theory yielding an accepted value for $\Delta_f H^o_0$ (CF_3), this has not been the case for the SF_5 radical where theory [47] and experiment [43] differ by over 70 kJ mol^{-1}. Using Irikura's value for $\Delta_f H^o_0$ (SF_5) [47], for example, Ball [30] predicts a S–C bond strength of 311 kJ mol^{-1}, much closer to our experimental value of 372 ± 43 kJ mol^{-1}. Xu *et al.* [33], using varying density functional methods but without zero point vibrational energy corrections, obtain dissociation energies for $SF_5CF_3 \rightarrow SF_5 + CF_3$ ranging between 1.9 and 3.1 eV

(*ca.* 180-300 kJ mol^{-1}). Whilst there are no atmospheric implications for SF_5CF_3 from these differing values for its enthalpy of formation, it is surprising and slightly concerning that experiment and theory differ by as much as 100 kJ mol^{-1}, *ca.* 1 eV, for a microscopic property as fundamental as the 0 K enthalpy of formation. State-of-the-art *ab initio* calculations on the SF_5–CF_3 bond strength are currently being performed with full configuration interaction and a much larger basis set than has been used to date [48]. The calculations are not yet complete, but early indications are that they predict an S–C bond strength much closer to the experimental value [20] than the earlier calculations.

5.4 *Threshold photoelectron spectrum of SF_5CF_3*

In the final two parts of section 5, I describe additional and important information on an isolated SF_5CF_3 molecule that resulted from this TPEPICO study. The valence threshold photoelectron spectrum (TPES) of SF_5CF_3 was measured from 12.7 to 26.4 eV with a resolution of 0.3 nm (Figure 7). No vibrational structure was observed. The onset of ionisation, defined as the energy at which signal is first observed above the background noise, is 12.92 ± 0.18 eV. The vertical ionisation energy of this first band occurs at 14.13 eV. The low value of this vertical IE, *ca.* 2 eV lower than that in both CF_4 and SF_6 where the HOMO has F 2pπ non-bonding character, has already been noted. The large difference between the onset of ionisation and the vertical IE suggests a significant change in geometry between neutral and cation, probably in the S–C bond length, compatible with a repulsive ground state of the parent cation along this coordinate. *Ab initio* calculations on the structure of SF_5CF_3 by Knowles [9] at the Hartree-Fock level were described briefly in Section 2. The predicted structure, detailed in the caption to Figure 1, is in good agreement with that from gas-phase electron diffraction [8]. No other structures of molecules with stoichiometry $C_1S_1F_8$ are stable. The HOMO of SF_5CF_3 has a large S–C σ-bonding character, whereas the next three orbitals lie *ca.* 2.7 eV lower in energy and are F 2pπ non-bonding in character. No minimum-energy geometry of the ground state of $SF_5CF_3^+$ can be obtained at either the Hartree-Fock or the MP2(full)/6-31g(d) level, giving further evidence that this state is indeed unbound. Results from these simple calculations have recently been confirmed using the GAMESS-UK suite of programs with a variety of basis sets [15]. Higher-energy peaks in the TPES are observed at 15.68, 16.94, 17.86, 19.44, 21.34, 22.01 and 24.67 eV. Attempts have now been made to assign these peaks in the TPES and how they correlate with peaks in the (T)PES of both CF_4 and SF_6 [15]. The evidence from the vacuum-UV absorption and valence photoelectron spectrum of SF_5CF_3 is that this molecule behaves more like a perturbed SF_6 than a perturbed CF_4 molecule [15].

5.5 *Ion yields and fixed-energy TPEPICO spectra of SF_5CF_3*

The time-of-flight spectrum of the fragment ions from SF_5CF_3, integrated over the whole range of VUV photoexcitation energies 12.7–26.4 eV, is shown in Figure 8. The parent ion is not observed. CF_3^+ and SF_3^+ are the dominant ions, then SF_5^+, with CF_2^+ and SF_4^+ being very weak. Table 2 shows threshold

energies for their production. We consider first the *major* ions, defined as those formed by a single bond cleavage ; reactions in which there is no barrier in the exit channel and hence, in the conventional sense, no transition state. The ion yield of CF_3^+ follows that of the TPES of SF_5CF_3 from the onset of ionisation to *ca.* 20 eV, and states of the parent ion with vertical energies below 20 eV dissociate predominantly to this ion. By contrast, the SF_5^+ signal is so weak that it is not possible to say whether its ion yield shows any correlation with electronic states of $SF_5CF_3^+$. Even well above the SF_5^+ threshold of 13.9 eV, its ion yield relative to that of CF_3^+ remains very weak. These thresholds and relative intensities are in good agreement with a tunable electron energy beam study over the same range of energies [22]. This behaviour is somewhat surprising for a large polyatomic cation with ten atoms and a correspondingly large density of vibronic states. These dissociation properties of $SF_5CF_3^+$ suggest that it behaves more like a psuedo-diatomic molecule with a much lower density of states, dissociating only on one repulsive potential energy surface with no curve crossings. By contrast, the *minor* ions are defined as those which can only form following intramolecular rearrangement within a transition state of the unimolecular reaction following photoexcitaton. The threshold energy for the strongest minor ion, SF_3^+, is 14.94 ± 0.13 eV. Energetically, it can only form at this energy if the accompanying neutral fragments are CF_4 + F. Likewise, the two very weak minor ions, SF_4^+ and CF_2^+, can only form at their thresholds (Table 2) if migration of F^- across the S–C bond occurs in the transition state to form CF_4 and SF_6, respectively. Such migrations in unimolecular reactions are usually only associated with H(D) atoms, but F-atom migration across a C–X bond has been observed in fragmentation of other long-lived greenhouse gases, *e.g.* the perfluorocarbon cations, $C_xF_y^+$ [49].

Table 3 shows values for the mean translational KE release into $CF_3^+ + SF_5$ when SF_5CF_3 is excited into the ground and first four excited states of the parent ion. The procedure is described in Section 5.2. Columns 5-7 show the experimental fractional release into translational energy ($f_{expt} = \langle KE \rangle_T / E_{avail}$) and the predictions of statistical [50] and pure-impulsive [42] models. It was noted in Section 5.3 that for dissociation of the ground state of $SF_5CF_3^+$, the value for f_{expt} at 14.25 eV, 0.21, is very close to that predicted by the pure-impulsive model. This is as expected, because the Franck-Condon maximum of the ground state of $SF_5CF_3^+$ lies *ca.* 1.3 eV higher than the dissociation threshold to $CF_3^+ + SF_5 + e^-$. Dissociation from this repulsive potential energy surface is therefore expected to occur rapidly on a sub-picosecond timescale, with a relatively large amount of the available energy being released into translation of the two fragments. As the photon energy increases to 19 eV, however, f_{expt} decreases by a factor of *ca.* 3-4. It appears that as higher-energy electronic states of $SF_5CF_3^+$ are populated, there is a reduced coupling of the initially-excited vibrational modes into the reaction coordinate, behaviour that is normally associated with a multi-atom polyatomic species. This phenomenon, that the value of $\langle KE \rangle_T$ does not increase as rapidly with photon energy as a pure-impulsive model would predict, has also been observed in dissociation reactions in other polyatomic molecules, CF_3^+ from CF_4 and SF_5^+ from SF_6 [51].

6. *Removal processes of SF_5CF_3 from the earth's atmosphere in the mesosphere*

The larger-than-expected value of the S–C bond strength [20] and the absence of excited electronic states of SF_5CF_3 lying below *ca.* 8 eV [23] led scientists to study processes in the mesosphere that could remove this greenhouse gas from the atmosphere ; reactions with cations, electrons and vacuum-UV photodissociation (the last three terms in the bracket of equ. (V)).

6.1 *Reactions of SF_5CF_3 with cations and anions*

Two papers have described the reactions of cations with SF_5CF_3 [52,53], one with anions [54]. All these studies have been made in a selected ion flow tube (SIFT), and a schematic of this apparatus is shown in Figure 9. Such an experiment can determine the rate coefficient and product ions and their branching ratios for the reactions of small anions or cations with neutral molecules, generically $A^{\pm} + BC \rightarrow D^{\pm} +$ EF where the ions can be atomic or molecular. Only fast reactions with rate coefficient greater than *ca.* 10^{-13} cm^3 $molecule^{-1}$ s^{-1} can be studied. In brief, a reagent ion of interest is produced in a high pressure electron impact ion source containing an appropriate source gas. The cation or anion is injected through a quadrupole mass filter into a flow tube holding *ca.* 0.5 Torr of high purity helium as a buffer gas. The neutral reactant of choice is then admitted through an inlet at one of various points down the flow tube. The resultant ionic products are detected using a quadrupole mass spectrometer. The loss of reagent ion signal, alongside the increase in the various product ion signal(s), is recorded as a function of neutral reactant concentration. The amount of neutral is altered between zero and a concentration that depletes the reactant ion signal by *ca.* 90 %. Since the experiment operates under pseudo-first-order conditions with $[A^{\pm}] \ll [BC]$, and with knowledge of the reaction length and ion flow velocity, a plot of the logarithm of the reagent ion signal *vs.* neutral molecule concentration allows the rate coefficient to be determined. Percentage branching ratios for each product ion are derived from graphs of the relative product ion counts *vs.* neutral molecule concentration, with extrapolation to zero neutral gas flow to allow for the effect of any secondary reactions. Most of the Birmingham, UK studies are made at 298 K, whereas the Air Force Research Laboratories, US apparatus can operate over the temperature range *ca.* 250-500 K.

Unrelated to the atmospheric importance of such reactions for SF_5CF_3, an additional motivation for such studies is to understand the importance of long-range charge transfer in cation-molecule reactions. Charge transfer can occur either at long range or at short range. In the long-range mechanism, assuming BC has a permanent dipole moment, A^+ and BC approach under the influence of their charge-dipole interaction, until at some critical distance (R_c) the A^+-BC and A-BC^+ potential energy curves cross. At this point an electron jump can take place. We have shown [55] that R_c depends on the difference in energy between the recombination energy (RE) of A^+ and the ionisation energy (IE) of BC ; the smaller

this difference, the larger R_c. (The RE is defined as the energy that is released when a cation forms its neutral compound.) Furthermore, two important factors for a rapid electron transfer and an efficient long-range charge transfer process are a non-zero energy resonance connecting BC to an electronic state of BC^+ at the RE of A^+, and the transferring electron comes from a molecular orbital of BC that is not shielded from the approaching cation. So long as there is some overlap of vibrational wavefunction between BC and BC^+ at the RE of A^+, the magnitude of the photoionisation Franck-Condon factor for BC is not as important as originally thought in determining the efficiency of such a reaction. We note that if this long-range charge transfer mechanism operates, then the branching ratios for fragmentation of $(BC^+)^{(*)}$, where (*) donates the possibility of BC^+ being in an excited electronic state, are expected to be independent of how this state is produced. Hence, we would expect similar product branching ratios from the ion-molecule study and from the TPEPICO photoionisation study, assuming the photon energy in the latter experiment matches the RE of A^+ in the former.

When long-range charge transfer is unfavourable, A^+ and BC move closer together. As their separation decreases, distortion of the potential energy surface of interaction occurs. Eventually, a curve crossing can occur through which efficient charge transfer takes place. This is called short-range charge transfer. As an intermediate complex has formed, a chemical reaction, defined as the breaking and making of new bonds, may, in addition, compete with short-range charge transfer. This means that it is unlikely that the product branching ratios from the ion-molecule and from the TPEPICO experiments will mimic each other. Thus, a comparison of the fragmentation patterns from the SIFT and TPEPICO experiments, together with an analysis of the TPES of BC at the energy of the RE of A^+, may indicate which mechanism, be it long-range or short-range, is dominant for the reaction of each cation. Agreement within *ca.* ±15 % is taken as evidence for possible long-range charge transfer [56]. We have made this comparison for the reactions of SF_5CF_3 with those cations whose concentrations are the highest in the mesosphere, and might therefore be expected to contribute to the removal of SF_5CF_3 from the earth's atmosphere.

The results of the SIFT study for reactions of SF_5CF_3 with the important atmospheric cations N_2^+, N^+, CO^+, CO_2^+, O^+, N_2O^+, H_2O^+ and O_2^+ are shown in Table 4. The RE values of these cations range from 15.58 (for N_2^+) to 12.07 eV (for O_2^+). The first five ions have RE values greater than the onset of ionisation of SF_5CF_3, so in principle long-range charge transfer may occur. The last three cations have RE values below the onset of ionisation, so can only react *via* a short-range process and the formation of a reaction intermediate. Seven of the eight ions react with a rate coefficient close to or equal to the Langevin capture value [57]. O_2^+ reacts significantly slower. The reactions of the six cations with RE in the range 12.89 to 15.58 eV (*i.e.* those equal to or greater than the onset of ionisation of SF_5CF_3) appear to occur by dissociative charge transfer, with CF_3^+ and SF_3^+ being the dominant product ions. It seems

likely that CF_3^+ forms by direct breaking of the S–C bond, whereas SF_3^+ may form from dissociation of $(SF_4^+)^*$ following intramolecular rearrangement within a reaction intermediate. The evidence for formation of such an intermediate lies in the SF_3^+ branching ratios. Significant values, *ca.* 10-20 %, are observed for reactions of N^+, CO^+, CO_2^+, O^+ and N_2O^+ despite the fact that these ions have RE values less than 14.94 eV, the appearance energy at 298 K (AE_{298}) of this cation in the photon-induced study (Section 5.5) [20]. Only the yield of SF_3^+ from the N_2^+ reaction, 28 %, gets close to approaching that from the photon-induced reaction at hν = 15.58 eV, 25 %. Note also that the SF_3^+ ion is dominant for the H_2O^+ reaction, 92 %, although this ion has an RE value 0.3 eV below the onset of ionisation of SF_5CF_3. Thus the evidence is that, with the possible exception of N_2^+, all reactions yielding SF_3^+ proceed *via* the formation of an intermediate at short range, followed by intramolecular re-arrangement and migration of F^- across the S–C bond to form CF_4 as an accompanying, thermochemically stable neutral partner. Table 4 also highlights the difficulties in using the experimental values of Fisher *et al.* [43] for the enthalpies of formation of $SF_x^{(+)}$, in that some 'fast' reactions are calculated to be significantly endothermic. Thus, column 5 of Table 4 also shows values for $\Delta_r H^o_0$ calculated using the theoretical values of Irikura [47] for $\Delta_f H^o_0\,(SF_x^{(+)})$, where his more negative values make such reactions exothermic.

In theory, the rate coefficients and products of such reactions should be used to model the fate of SF_5CF_3 in the mesosphere and hence its atmospheric lifetime. However, despite the fact that these reactions are fast, *ca.* 10^{-9} cm^3 $molecule^{-1}$ s^{-1}, they are still over an order of magnitude slower than low-energy electron attachment (Section 6.2). Furthermore, the concentrations of such positive ions in the mesosphere are also at least an order of magnitude lower than that of free electrons [58]. Therefore, the reactions of both cations and anions with SF_5CF_3, whilst yielding a huge amount of information at the microscopic level, makes very litle contribution to the atmospheric chemistry of this molecule, because the reactions are too slow and the ion concentrations too low ; the third term in the bracket in the right-hand side of equ. (V) is negligibly small. Although this section has concentrated on the reactions of *cations* with SF_5CF_3, mainly because of the comparison with the TPEPICO data and hence an understanding of reaction mechanisms, the arguments in this paragraph also hold true for the reactions of *anions* with SF_5CF_3.

6.2 *Reactions of SF_5CF_3 with low-energy electrons*

Since the mesosphere is electrically neutral, the total concentration of positive ions must be balanced by that of anions and free electrons, and Adams and Smith [58] estimate a mean electron number density of 10^5 cm^{-3} for altitudes in the range $100 < h < 200$ km, falling rapidly to 10^3 cm^{-3} for $h \approx 80$ km. The mesosphere is thermalised with a temperature in the range 170 to 250 K, the lowest temperature occuring at the mesopause, $h \approx 85$ km. The average thermal energy of the electrons, $3k_BT/2$, is therefore low, *ca.*

0.02–0.03 eV, and laboratory studies of low-energy electron attachment to SF_5CF_3 can give an important guide to reactions that may occur in the mesosphere.

Several groups have made such measurements. The group of Mayhew in Birmingham, UK [59] uses a Swarm apparatus to determine absolute electron attachment cross-sections, rate coefficients and the products of the low-energy attachment. The Air Force Research Laboratory group of Viggiano [32] use a flowing afterglow Langmuir probe (FALP) apparatus whose temperature can be controlled between *ca.* 300-550 K. They can also measure the rate coefficient for low-energy electron attachment and the products of such reactions. Both give near-identical results for SF_5CF_3. Mayhew and Kennedy [59] measure the thermal attachment rate coefficient to be $7.7 \pm 0.6 \times 10^{-8}$ cm^3 molecule^{-1} s^{-1}, with the only anionic product being SF_5^-. Miller *et al.* [32] measure the rate coefficient at 296 K to be slightly higher, $8.6 \pm 2.2 \times 10^{-8}$ cm^3 molecule^{-1} s^{-1}, the rate constant increasing very slightly with increasing temperature giving an Arrhenius activation barrier of 25 meV or 2.4 kJ mol^{-1}. Again, the only observed charged product is SF_5^-. The groups of Illenberger (Berlin, Germany) [25] and Märk (Innsbruck, Austria) [26] operate under collision-free beam conditions and use a tunable electron beam with energies in the range *ca.* 0-15 eV. Absolute cross-sections and rate coefficients cannot be determined, but the presence of low-energy resonances leading to the production of certain anions can be measured. For SF_5CF_3, both beam studies show a large dissociative electron attachment cross section at 0 eV to form $SF_5^- + CF_3$, in excellent agreement with the Swarm and FALP studies. The 0 eV CF_3^- peak is over four orders of magnitude weaker [25]. Of less importance to the atmospheric chemistry of SF_5CF_3, absolute cross sections for electron scattering at much higher electron energies, 100-10,000 eV, have been measured [24].

A schematic of the Birmingham Swarm apparatus, described in detail elsewhere [60], is shown in Figure 10. The source of electrons is a radioactive ^{63}Ni β-emitting sample which is located in front of a drift tube. An electric potential can be applied along this drift tube, creating a uniform electric field, *E*, which draws electrons towards a Faraday plate detector. An electron energy distribution is established, determined by a dynamic balance between the kinetic energy gained from the electric field and energy loss through multiple collisions with the high-pressure buffer gas (either Ar or N_2, number density *N*). Anions formed by electron attachment can be distinguished from electrons by a simple timing arrangement in which the electrons are admitted into the drift tube as a short (*ca.* 1 ms) pulse *via* an electron gate. By monitoring the attenuation of electron pulses as a function of the reactant gas concentration, the density-reduced electron attachment coefficient, α, is determined as a function of *E/N*. Multiplication of α by the mean electron drift speed gives the electron attachment rate constant, k_a, again as a function of *E/N*. A small hole in the Faraday plate allows anions formed within the drift tube to enter a differentially-pumped region and a quadrupole mass spectrometer. The product anions formed from

electron attachment can thus be determined, the major advantage of this instrument compared to more conventional electron swarm apparatus [61].

Using Ar or N_2 buffer gas, electrons in the Swarm apparatus have a non-thermal energy distribution. However, many detectors commercially used for the detection of electronegative molecules rely on *thermal* electron attachment in high-pressure buffer gas. Furthermore, if the concentration of an electron-attaching gas is to be accurately determined, thermal attachment rate coefficients are needed. Until recently, we could only obtain such rate coefficients, such as for SF_5CF_3 [59], by extrapolation of our data to zero electric field strengths (Figure 11). We have now developed a new drift tube ideally suited for thermal electron attachment in a high pressure (*ca.* 1 bar) of CO_2 buffer gas, and confirmed its correct mode of operation with SF_6 where α is now determined to be independent of *E/N* [62].

The electron attachment rate coefficient for SF_5CF_3, $7.7 \pm 0.6 \times 10^{-8}$ cm^3 molecule^{-1} s^{-1}, is fast, but significantly slower than that for SF_6, $2.38 \pm 0.15 \times 10^{-7}$ cm^3 molecule^{-1} s^{-1} [62], which is close to the theoretical maximum for pure *s*-wave capture [63]. From an atmospheric point of view, however, perhaps the most important result is that the product of such low-energy electron attachment to SF_5CF_3 is not the parent anion, but a fragment anion SF_5^-. Assuming SF_5CF_3 is not recycled by subsequent reactions of SF_5^-, low-energy electron attachment is therefore one route to remove SF_5CF_3 from the earth's atmosphere, and the pseudo-first-order rate constant for this process, the fourth term in the bracket on the right-hand side of equ. (V), will be significant. Energetically, this removal process is also possible. Table 5 shows that, within the error for $\Delta_f H^o_0$ (SF_5CF_3) quoted in Section 5.3, the reaction $SF_5CF_3 + e^-$ (0 eV) $\rightarrow SF_5^- + CF_3$ is exothermic, using both the 0 K enthalpy of formation for SF_5CF_3 from experiment [20] and the less negative value from theory [32]. Using either value for $\Delta_f H^o_0$ (SF_5CF_3), formation of $CF_3^- + SF_5$ is significantly endothermic, explaining the almost total absence of this anion in the zero eV peak in the electron beam studies [25,26].

6.3 *Reactions of SF_5CF_3 with vacuum-UV photons, especially Lyman-α (121.6 nm) radiation*

The VUV absorption spectrum of SF_5CF_3, including a determination of the absorption cross section at the Lyman-α wavelength of 121.6 nm, has been measured by five groups using either direct absorption and the Beer-Lambert law [4,16,17] or a double-ion chamber [15,18]. Measurements have been made using VUV laser radiation [17], fixed-energy lamp sources [18], and tunable VUV radiation from a synchrotron [4,15-17]. The synchrotron experiments have been performed with wavelengths both above [4,17] and below [15,16] the lithium fluoride window cutoff of *ca.* 105 nm (or 11.8 eV). The apparatus used by the Birmingham group, described in detail by Hoxha *et al.* [64] and used at both the Bessy-I, Berlin and SuperAco, Paris synchrotron sources, is shown in Figure 12.

In brief, radiation from the synchrotron passes through the exit slit of a VUV monochromator (a 1.5 m normal-incidence at Bessy-I), a two-stage differential pumping section, and a 1 mm thick stainless steel microchannel plate into an absorption cell of length, L, 300 mm. A pressure differential of 1000:1 across the microchannel plate is possible. This plate can transmit wavelengths well below 100 nm, so this experiment can measure absorption spectra below the LiF cutoff, and yet the path length of the absorption 'cell' is defined. The gas pressure in the absorption cell, in the range 5-60 μbar, is maintained constant *via* a slow controlled flow of gas. The VUV radiation at the end of the cell is detected through a sodium-salicylate-coated window and a visible photomultiplier tube. Since the pressure of gas and optical path length are known, measurement of the ratio of transmitted intensity observed for background (no gas) and sample spectra (with gas) can yield, *via* the Beer Lambert law $ln(I_o/I) = \sigma cL$, absolute absorption cross sections, σ, in units of cm^2 $molecule^{-1}$; c is the number density of the gas in units of molecules cm^{-3}, and L has units of cm. In the calculation of I_o/I at every value of the VUV energy, allowance is made for the natural decay of the VUV flux over the time of an experiment. No allowance is made for the small pressure gradient within the absorption cell due to gas leakage through the microchannel plate, and the small effects of second-order radiation from the VUV monochromator are ignored. We estimate that cross sections are accurate to *ca.* 15-20 %, and the ignorance of second-order effects may make this error greater at wavelengths close to twice the blaze wavelength of the grating in the VUV monochromator. Absorption spectra in the range *ca.* 50-200 nm at a resolution of better than 0.1 nm can routinely be measured. The range of cross sections that can be determined span *ca.* 10^{-16} to 10^{-20} cm^2. The absorption spectrum of SF_5CF_3 measured with this apparatus is shown in Figure 13 [16], and the cross section at 121.6 nm is determined to be $1.3 \pm 0.2 \times 10^{-17}$ cm^2 (or 13 ± 2 Mb) ; note that, following a re-analysis of the data, this value is 2 Mb lower than that reported in [16]. This value is significantly greater than that for SF_6 where $\sigma_{121.6}$ is 1.76×10^{-18} cm^2, and orders of magnitude greater than for CF_4 which shows negligible absorption at this wavelength ($\sigma_{121.6} < 8 \times 10^{-22}$ cm^2) [65]. As commented in Section 5.4, the evidence from the assignment of the absorption spectrum by Holland *et al.* [15] is that SF_5CF_3 behaves more like SF_6 than CF_4 in its VUV photoabsorption properties. The value of $\sigma_{121.6}$ from Chim *et al.* [16] is slightly higher than that determined by others. Holland *et al.* [15], Takahashi *et al.* [17] and Limao-Vieira [4] obtain 6.4, 7.8 and 6.5 Mb, respectively, and the result of Chim *et al.* may be anomalously high because higher-order effects are ignored. That said, using the known value of $J_{121.6}$ [66], the absolute value of this cross section makes negligible difference to the lifetime of SF_5CF_3 in the mesosphere, because VUV photodissociation only contributes *ca.* 1 % to the removal of SF_5CF_3 by processes that occur in the mesosphere (Section 7).

As with the states of $SF_5CF_3^-$ excited by low-energy electrons, VUV photoabsorption will only contribute to the removal of SF_5CF_3 from the atmosphere if the valence or Rydberg electronic states photoexcited at 121.6 nm are dissociative. The bottom half of Table 5 shows that whilst dissociation to neutral SF_5 and CF_3 is clearly energetically possible since the SF_5–CF_3 bond strength is only 3.86 eV (Section 5.3), dissociation to the ion pair $CF_3^+ + SF_5^-$ (but not to $SF_5^+ + CF_3^-$) can also occur with 10.2 eV photon excitation. In determining the energetics of these reactions, we use values for the electron affinity of the CF_3 and SF_5 radicals of 1.82 and 3.8 eV, respectively [67,68]. Although the quantum yields for dissociation into ion pairs are generally unknown, their formation following VUV photoexcitation of polyatomic molecules should be prevalent, but this process for SF_5CF_3 has not yet been observed.

Table 6 summarises the electron attachment rate coefficient and Lyman-α absorption cross section for SF_5CF_3, SF_6 and CF_4 ; reactions of these molecules with small cations and anions are not included as these processes make negligible contribution to their removal from the mesosphere. It is clear that SF_5CF_3 behaves much more like a modified SF_6 than a modified CF_4 molecule. The electron attachment rate coefficient for SF_5CF_3 is *ca.* 3 times slower than that for SF_6, $\sigma_{121.6}$ is *ca.* 7 times larger, but k_e and $\sigma_{121.6}$ for CF_4 are orders of magnitude smaller. The only aspect of the photochemistry of SF_5CF_3 where it behaves like a modified CF_4 molecule is its vacuum-UV fluorescence properties. Following VUV photoexcitation in the range 8–25 eV, weak UV/visible emission is observed from CF_3, CF_2 and possibly the parent ion in the energy ranges *ca.* 10-12, 15-17 and hν > 20 eV [70]. In this aspect, SF_5CF_3 appears to behave like the group of molecules CF_3X (X = H,F,Cl,Br) [71]. This work does not relate to the atmospheric chemistry of SF_5CF_3, but will be described in detail in a future publication [70].

7. *Lifetime of SF_5CF_3 in the earth's atmosphere and conclusions*

The lifetime of a pollutant or greenhouse gas is a term that can mean different things to different people, and confusion can sometimes arise [72]. To a laboratory-based physical chemist, the lifetime usually means the inverse of the pseudo-first-order rate constant of the dominant chemical or photolytic process that removes the pollutant from the atmosphere. Using CH_4 as an example, it is predominantly removed in the troposphere *via* oxidation by the OH free radical, $OH + CH_4 \rightarrow H_2O + CH_3$. The rate coefficient for this reaction at 298 *K* is 6.39×10^{-15} cm^3 molecule^{-1} s^{-1} [73], so the lifetime is approximately equal to $(k_{298}[OH])^{-1}$. Using an average value for the tropospheric OH concentration of 10^6 molecules cm^{-3}, the atmospheric lifetime of CH_4 is calculated to be *ca.* 5 years. This is within a factor of 2.4 of the accepted value of 12 years (Table 1). The difference arises because CH_4 is not emitted uniformly from the earth's surface, a finite time is needed to transport CH_4 *via* convection and diffusion into the troposphere, and oxidation occurs at different altitudes in the troposphere where the concentration of OH will vary from its average value of 10^6 molecules cm^{-3}. In simple terms, this is an example of a two-step kinetic process, A

$\rightarrow$ B $\rightarrow$ C with first-order rate constants k_1 and k_2. The first step, A $\rightarrow$ B, defines the transport of the pollutant into the atmosphere, whilst the second step, B $\rightarrow$ C, defines the chemical or photolytic process (*e.g.* reaction with an OH radical in the troposphere, electron attachment in the mesosphere) that removes the pollutant from the atmosphere. In general, the overall rate of the process (whose inverse is called the *lifetime*) will be a function of both k_1 and k_2, but its value will be dominated by the *slower* of the two steps. Thus, in writing the lifetime of CH_4 simply as $(k_{298}[OH])^{-1}$, we are assuming that the first step, transport into the region of the atmosphere where chemical reactions occurs, is infinitely fast.

SF_5CF_3, perfluorocarbons such as CF_4, and SF_6 behave in the opposite sense. The slow, rate-determining process is now the first step, transport of the greenhouse gas from the surface of the earth into the mesosphere, and the chemical or photolytic processes that remove SF_5CF_3 *etc.* in the mesosphere will have very little influence on the lifetime. We can define a chemical lifetime, $\tau_{chemical}$, as $(k_e[e^-] + \sigma_{121.6}J_{121.6})^{-1}$, assuming the quantum yield for dissociation at 121.6 nm is unity, but the value will be a function of position, particularly altitude, in the atmosphere. In the troposphere, $\tau_{chemical}$ will be infinite because both the concentration of electrons and $J_{121.6}$ are effectively zero at low altitude, but in the mesosphere $\tau_{chemical}$ will be much less. In other words, multiplication of k_e for SF_5CF_3 *etc.* by a typical electron density in the mesosphere, *ca.* 10^4 cm^{-3} [58], yields a chemical lifetime which is far too small and bears no relation to the true atmospheric lifetime, simply because most of the SF_5CF_3 *etc.* does not reside in the mesosphere.

The global atmospheric lifetime is obtained from globally-averaged loss frequencies. In forming the average, the psuedo-first-order destruction rate coefficient for each region of the atmosphere is weighted according to the number of molecules of compound in that region,

$$\langle k \rangle_{global} = \frac{\sum_i k_i V_i n_i}{\sum_i V_i n_i} \qquad \text{(IX)}$$

where i is a region, k_i is the pseudo-first-order rate coefficient for region i, V_i is the volume of region i, and n_i is the number density of the greenhouse gas under study in region i. The averaging process thus needs input from a 2-D or 3-D model of the atmosphere in order to supply the values of n_i. This is essentially a meterological problem, and may explain why such scientists and physical chemists sometimes have different interpretations of what the lifetime of a greenhouse gas actually means. The only sensible definition is the inverse of $\langle k \rangle_{global}$. Many such studies have been made for SF_6 [65,74,75], and differences in the kinetic model (k_i) and the atmospheric distributions (n_i) from different climate or

transport models account for the variety of atmospheric lifetimes that have been reported. For molecules such as SF_6 (and SF_5CF_3) which are only destroyed in the mesosphere above 60 km, the importance of both these factors has been explored by Hall and Waugh [76]. Their results show that because the fraction of the total number of SF_6 molecules in the mesosphere is very small, the global atmospheric lifetime is very much longer than the mesospheric, chemical lifetime. Thus, they quote that if the mesospheric loss frequency is 9×10^{-8} s^{-1}, corresponding to a local lifetime of 129 days, then the global lifetime ranges between 1424 and 1975 years, according to which climate or transport model is used. In conclusion, therefore, the lifetime of SF_6, SF_5CF_3 and CF_4 is dominated by the meterology that transports these pollutants into the mesosphere, but the fate of each molecule when it reacts with low-energy electrons and Lyman-α radiation may make a small contribution to $\langle k \rangle_{global}$.

To the author's knowledge, no full meterological analysis of SF_5CF_3 in the atmosphere has been performed. SF_6 and SF_5CF_3 both attach electrons with a fast rate coefficient ($> 10^{-8}$ cm^3 $molecule^{-1}$ s^{-1}) and show significant absorption with Lyman-α radiation. Furthermore, the height profiles of SF_6 and SF_5CF_3 are similar in the atmosphere [1]. It should therefore be appropriate to make quantitative comparisons between these two molecules, expecting them to have similar lifetimes in the atmosphere. By contrast, the almost infinite value for the lifetime of CF_4, greater than 50,000 years [65,77], arises because this molecule shows no absorption at 121.6 nm [65] and attaches electrons at a negligibly slow rate [69]. k_e for SF_5CF_3 at 298 K is 3.1 times smaller than for SF_6, whereas the absorption cross-section is 7.4 times larger (Table 6). Therefore, the pseudo-first-order rate constant for removal of SF_5CF_3 by electrons divided by that due to photons at the same altitude of the mesosphere, $k_e[e^-] / \sigma_{121.6}J_{121.6}$, is 22.9 times smaller than this ratio for SF_6. (This calculation assumes that electron attachment to both SF_6 and SF_5CF_3 leads only to the formation of a fragment anion, SF_5^-, which is not recycled.) Assuming an incorrect value for k_e of 1×10^{-9} cm^3 $molecule^{-1}$ s^{-1}, Ravishankara *et al.* [65] initially determined that this ratio of pseudo-first-order rate constants for SF_6 was 3.2, and obtained an atmospheric lifetime of 3200 years. Using the much larger and correct value for k_e (SF_6) of 2.3×10^{-7} cm^3 $molecule^{-1}$ s^{-1}, Morris *et al.* [74] showed that this ratio of pseudo-first-order rate constants was 1998, and determined a lower limit to the atmospheric lifetime of 800 years. The lower limit arises because they assumed that every electron attachment event led to the permanent removal of SF_6 from the atmosphere. Reddmann *et al.* [75] considered a number of scenarios for the destruction of SF_6^-. They found that if less than 100 % was destroyed, the lifetime, not surprisingly, increased. They calculated values spanning 400 to 10000 years, depending on the loss mechanism and the value for the electron density in the upper stratosphere / mesosphere.

Assuming that the analysis of Morris *et al.* [74] for SF_6 is correct, then the predominant removal process for SF_5CF_3 remains electron attachment and not VUV photolysis, since the ratio of the pseudo-first-order

rate constants for SF_5CF_3 is 1998 / 22.9 or 87.2, *i.e.* still much greater than unity. Without a full meterological study, however, as explained above it is very difficult to convert these first-order rate constants into a global lifetime for SF_5CF_3. What can be said is that, *per molecule*, the quantum yield for electron attachment to SF_5CF_3 in the mesosphere is 87.2/88.2 or 0.989, and for Lyman-α photodissociation 1/88.2 or 0.011. The atmospheric lifetime is dominated by the meterology that transports SF_5CF_3 to the upper altitudes of the atmosphere and is likely to be *ca.* 1000 years, with an uncertainty in this number possibly as large as ± 300 years.

In conclusion, it is quite clear that, whilst the current concentrations of SF_5CF_3 in the atmosphere are still very low, mankind is stuck with this problem for a very long time. Since the original paper by Sturges *et al*. was published five years ago [1], a huge amount of fundamental research has meant that the atmospheric properties and reactions of SF_5CF_3 are now well understood, and further research effort will only contribute at the edges to understand the environmental impact of this greenhouse gas. It is suggested that reliable monitors, probably using the IR absorption properties of this molecule, are installed to determine the concentration of SF_5CF_3 both at the earth's surface and in the atmosphere. It is also suggested that policymakers should be concerned at the high annual growth rate of SF_5CF_3, and measures should be put in place world-wide to control its emissions.

Acknowledgements

I thank members of my research group who participated in our laboratory-based experiments on SF_5CF_3, and EPSRC, UK and the EU for funding. I particularly thank Professor K P Shine, Reading University UK, for recent discussions on radiative forcing and global warming potentials, and Dr C R Howle, Bristol University UK, for a critical reading of the manuscript.

References

[1] W.T. Sturges, T.J. Wallington, M.D. Hurley, K.P. Shine, K. Sihra, A. Engel, D.E. Oram, S.A. Penkett, R. Mulvaney, C.A.M. Brenninkmeijer,
A potent greenhouse gas identified in the atmosphere : SF_5CF_3,
Science, 2000, **289**, 611-613.

[2] J.S. Chickos and W.E. Acree,
Enthalpies of vaporisation of organic and organometallic compounds, 1880-2002,
J. Phys. Chem. Ref. Data, 2003, **32**, 519-878.

[3] L. Huang, L. Zhu, X. Pan, J. Zhang, B. Ouyang, H. Hou,
One potential source of the potent greenhouse gas SF_5CF_3 : the reaction of SF_6 with fluorocarbons under discharge,
Atmos. Environ., 2005, **39**, 1641-1653.

[4] P. Limao-Vieira, S. Eden, P.A. Kendall, N.J. Mason, A. Giuliani, J. Heinesch, M.J. Hubin-Franskin, J. Delwiche, S.V. Hoffmann,

An experimental study of SF_5CF_3 by electron energy loss spectroscopy, VUV photo-absorption and photoelectron spectroscopy,
Int. J. Mass Spectrom., 2004, **233**, 335-341.

[5] N.J. Mason, A. Dawes, R. Mukerji, E.A. Drage, E. Vasekova, S.M. Webb and P. Limao-Vieira,
Atmospheric chemistry with synchrotron radiation,
J. Phys. B., 2005, **38**, S893-S911.

[6] A. McCulloch,
Fluorocarbons in the global environment : a review of the important interactions with atmospheric chemistry and physics,
J. Fluorine Chem., 2003, **123**, 21-29.

[7] P. Kisliuk, G.A. Silvey,
The microwave spectrum of SF_5CF_3,
J. Chem. Phys., 1952, **20**, 517-517.

[8] C.J. Marsden, D. Christen and H. Oberhammer,
The trans influence of CF_3 : gas-phase structure of SF_5CF_3,
J. Mol. Struct., 1985, **131**, 299-307.

[9] P.J. Knowles,
private communication, 2005.

[10] D.F. Eggers, H.E. Wright, D.W. Robinson,
The infrared spectrum of SF_5CF_3,
J. Chem. Phys., 1961, **35**, 1045-1050.

[11] J.E. Griffiths,
The infrared and Raman spectra of SF_5Cl and SF_5CF_3,
Spectrochim Acta A, 1967, **23**, 2145-2157.

[12] O.J. Nielsen, F.M. Nicolaisen, C. Bacher, M.D. Hurley, JT.J. Wallington, K.P. Shine,
Infrared spectrum and global warming potential of SF_5CF_3,
Atmos. Environ., 2002, **36**, 1237-1240.

[13] P.A. Kendall, N.J. Mason, G.A. Buchanan, G. Marston, P. Tegeder, A. Dawes, S. Eden, P. Limao-Vieira, D.A. Newnham,
Temperature dependent high-resolution infrared photoabsorption cross-sections of SF_5CF_3,
Chem. Phys., 2003, **287**, 137-142.

[14] C.P. Rinsland, S.W. Sharpe, R.L. Sams,
Temperature-dependent absorption cross-sections in the thermal infrared bands of SF_5CF_3,
J. Quant. Spec. Rad. Transfer, 2003, **82**, 483-490.

[15] D.M.P. Holland, D.A. Shaw, I.C. Walker, I.J. McEwen, E. Apra, M.F. Guest,
Study of the valence shell photoelectron and photoabsorption spectra of SF_5CF_3,
J. Phys. B., 2005, **38**, 2047-2067.

[16] R.Y.L. Chim, R.A. Kennedy, R.P. Tuckett,
The vacuum-UV absorption spectrum of SF_5CF_3 ; implications for its lifetime in the earth's atmosphere,
Chem. Phys. Letts., 2003, **367**, 697-703.

[17] K. Takahashi, T. Nakayama, Y. Matsumi, S. Solomon, T. Gejo, E. Shigemasa, T.J. Wallington,
Atmospheric lifetime of SF_5CF_3,
Geophys. Res. Letts., 2002, **29**, 1712-1715.

[18] P.A. Hatherly, A.J. Flaxman,
On the absolute absorption cross-section of SF_5CF_3,
Chem. Phys. Letts., 2003, **380**, 512-515.

[19] T. Ibuki, Y. Shimada, S. Nagaoka, A. Fujii, M. Hino, T. Kakiuchi, K. Okada, K. Tabayashi, T. Matsudo, Y. Yamana, I.H. Suzuki, Y. Tamenori,
Total photoabsorption cross-sections of SF_5CF_3 in the C, F and S *K*-shell regions,
Chem. Phys. Letts., 2004, **392**, 303-308.

[20] R.Y.L. Chim, R.A. Kennedy, R.P. Tuckett, W. Zhou, G.K. Jarvis, D.J. Collins, P.A. Hatherly,
Fragmentation of energy-selected $SF_5CF_3^+$ probed by threshold photoelectron photoion coincidence spectroscopy : bond dissociation energy of SF_5–CF_3 and its atmospheric implications,
J. Phys. Chem. A., 2001, **105**, 8403-8412.

[21] R.Y.L. Chim, R.A. Kennedy, R.P. Tuckett, W. Zhou, G.K. Jarvis, C.A. Mayhew, D.J. Collins, P.A. Hatherly,
Determination of the first dissociative ionisation energy of polyatomic molecules by TPEPICO Spectroscopy : application to CF_4, SF_6, SeF_6, TeF_6 and SF_5CF_3,
Surf. Rev. Letts., 2002, **9**, 129-135.

[22] B. Gstir, G. Hanel, J. Fedor, M. Probst, P. Scheier, N.J. Mason, T.D. Märk,
Electron impact ionisation studies of SF_5CF_3,
J. Phys. B., 2002, **35**, 2567-2574.

[23] P.A. Kendall, N.J. Mason,
Excitation and relative differential oscillator strengths for trifluoromethyl sulphur pentafluoride, SF_5CF_3, in the UV-VUV region by electron energy loss spectroscopy,
J. Elec. Spec. Rel. Phen., 2001, **120**, 27-31.

[24] P. Limao-Vieria, F. Blanco, J.C. Oller, A. Munoz, J.M. Perez, M. Vinodkumar, G. Garcia, N.J. Mason,
Electron scattering cross sections for SF_6 and SF_5CF_3 at intermediate and high energies (100-10,000 eV),
Phys. Rev. A., 2005, **71**, 0327201-0327206.

[25] R. Balog, M. Stano, P. Limao-Vieira, C. König, I. Bald, N.J. Mason, E. Illenberger,
Low energy electron interaction with free and bound SF_5CF_3 :
negative ion formation from single molecules, clusters and nanofilms,
J. Chem. Phys., 2003, **119**, 10396-10403.

[26] W. Sailer, H. Drexel, A. Pelc, V. Grill, N.J. Mason, E. Illenberger, J.D. Skalny, T. Mikoviny, P. Scheier, T.D. Märk,
Low energy electron attachment to SF_5CF_3,
Chem. Phys. Letts., 2002, **351**, 71-78.

[27] F. Pepi, A. Ricci, M. Di Stefano, M. Rosi,
Gas phase protonation of trifluoromethyl sulphur pentafluoride,
Phys. Chem. Chem. Phys., 2005, **7**, 1181-1186.

[28] T. Ibuki, Y. Shimada, R. Hashimoto, S. Nagaoka, M. Hino, K. Okada, I.H. Suzuki, Y. Morishita, Y. Tamenori,
Photofragmentation of C, F and S *K*-shell excited SF_5CF_3 studied by PEPICO and PIPICO spectroscopy,
Chem. Phys., 2005, **314**, 119-126.

[29] M.W. Chase,
NIST-JANAF thermochemical tables, 4th edition,
J. Phys. Chem. Ref. Data, 1998, monograph no.9.

[30] D.W. Ball,
Formation and vibrational spectrum of trifluoromethyl sulphur pentafluoride, SF_5CF_3, a new greenhouse gas : Gaussian-2 and Gausian-3 calculations,
J. Mol. Struct. (Theochem), 2002, **578**, 29-34.

[31] Z. Li, J. Yang, J.G. Hou, Q. Zhu,
Hybrid density functional study of SF_5CF_3
Chem. Phys. Letts., 2002, **359**, 321-325.

[32] T.M. Miller, S.T. Arnold, A.A. Viggiano, W.B. Knighton,
Electron attachment to SF_5CF_3 (296-563 *K*), and calculations of the neutral and anion thermochemistry,
J. Chem. Phys., 2002, **116**, 6021-6027.

[33] W. Xu, C. Xiao, Q. Li, Y. Xie and H.F. Schaefer,
Structures, thermochemistry, vibrational frequencies and integrated infrared intensities of SF_5CF_3 and $SF_5CF_3^-$, with implications for global temperature patterns,
Mol. Phys., 2004, **102**, 1415-1439.

[34] M. Turki, W. Eisfeld,
Theoretical investigation of the absorption and ionisation spectrum of the super greenhouse gas SF_5CF_3,
Phys. Chem. Chem. Phys., 2005, **7**, 1700-1708.

[35] *Intergovernmental Panel on Climate Change*, 3rd report, 2001, chapter 6.

[36] K. Sihra, M.D. Hurley, K.P. Shine, T.J. Wallington,
Updated radiative forcing estimates of 65 halocarbons and nonmethane hydrocarbons,
J. Geophys. Res., 2001, **106**, 20493-20505.

[37] http://www.earthfuture.com/stormyweather/greenhouse/

[38] K.P. Shine, J.S. Fuglestvedt, K. Hailemariam, N. Stuber,
Alternatives to the global warming potential for comparing climate impacts of emissions of greenhouse gases,
Climatic Change, 2005, **68**, 281-302.

[39] http://webbook.nist.gov/

[40] G.A. Garcia, P.M. Guyon, I. Powis,
The ionisation energy of CF_3 deduced from photoionisation of jet-cooled CF_3Br,
J. Phys. Chem. A., 2001, **105**, 8296-8301.

[41] D.P. Seccombe, R.Y.L. Chim, G.K. Jarvis, R.P. Tuckett,

The use of threshod photoelectron - photoion coincidence spectroscopy to probe the spectroscopic and dynamic properties of valence states of CCl_3F^+, CCl_3H^+ and CCl_3Br^+, *Phys. Chem. Chem. Phys.,* 2000, **2**, 769-780.

[42] K.E. Holdy, L.C. Klotz, K.R. Wilson,
Molecular dynamics of photodissociation : quasi-diatomic model for ICN,
J. Chem. Phys., 1970, **52**, 4588-4598.

[43] E.R. Fisher, B.L. Kickel, P.B. Armentrout,
Collision-induced dissociation and charge-transfer reactions of SF_x^+ (x=1-5) ; thermochemistry of sulphur fluoride ions and neutrals,
J. Chem. Phys., 1992**, 97**, 4859-4870.

[44] P.A. Hatherly, M. Stankiewicz, K. Codling, J.C. Creasey, H.M. Jones, R.P. Tuckett,
A threshold electron analyser for use in coincidence experiments,
Meas. Science and Tech., 1992, **3**, 891-896.

[45] I. Powis, P.I. Mansell, C.J. Danby,
Photoelectron photoion coincidence spectrometer for the study of translational energy release distributions,
Int. J. Mass Spectrom. Ion Phys., 1979, **32**, 15-26.

[46] G.K. Jarvis, D.P. Seccombe, R.P. Tuckett,
The effects of isotopomers in the state-selected photofragmentation of BCl_3^+, PCl_3^+ and PBr_3^+,
Chem. Phys. Letts., 1999, **315**, 287-292.

[47] K.K. Irikura,
Structure and thermochemistry of sulphur fluorides SF_n and their ions SF_n^+ (n = 1-5)
J. Chem. Phys., 1995, **102**, 5357-5367.

[48] M. Hanrath, S.D. Peyerimhoff and R.P. Tuckett,
unpublished data.

[49] G.K. Jarvis, K.J. Boyle, C.A. Mayhew, R.P. Tuckett,
Threshold photoelectron photoion coincidence spectroscopy of saturated perfluorocarbons C_2F_6, C_3F_8 and n-C_4F_{10},
J. Phys. Chem. A., 1998, **102**, 3219-3229.

[50] C.E. Klots,
Thermochemical and kinetic information from metastable decomposition of ions,
J. Chem. Phys., 1973, **58**, 5364-5367.

[51] J.C. Creasey, H.M. Jones, D.M. Smith, R.P. Tuckett, P.A. Hatherly, K. Codling, I. Powis,
Fragmentation of valence electronic states of CF_4^+ and SF_6^+ studied by threshold photoelectron photoion coincidence spectroscopy,
Chem. Phys., 1993, **174**, 441-452.

[52] C. Atterbury, R.A. Kennedy, C.A. Mayhew, R.P. Tuckett,
A study of the reactions of trifluoromethly sulphur pentafluoride, SF_5CF_3, with several positive ions of atmospheric interest,
Phys. Chem. Chem. Phys., 2001, **3**, 1949-1953.

[53] C. Atterbury, A.D.J. Critchley, R.A. Kennedy, C.A. Mayhew, R.P. Tuckett,
A study of the gas-phase reactions of several cations with two derivatives of SF_6 :

SF_5CF_3 and SF_5Cl,
Phys. Chem. Chem. Phys., 2002, **4**, 2206-2223.

[54] S.T. Arnold, T.M. Miller, A.A. Viggiano, C.A. Mayhew,
A temperature-dependent selected ion flow tube study of anions reacting with SF_5CF_3,
Int. J. Mass Spectrom., 2003, **223**, 403-409.

[55] G.K. Jarvis, R.A. Kennedy, C.A. Mayhew, R.P. Tuckett,
Chrge transfer from neutral perfluorocarbons to various cations :
long-range versus short-range reaction mechanisms
Int. J. Mass Spectrom., 2000 ,**202**, 323-343.

[56] M.A. Parkes, R.Y.L. Chim, C.A. Mayhew, V.A. Mikhailov, R.P. Tuckett,
Threshold photoelectron photoion coincidence spectroscopy and selected ion flow tube reactions of CHF_3 : comparison of product branching ratios,
Mol. Phys., 2006, in press.

[57] G. Gioumousis, D.P. Stevenson,
Reactions of gaseous molecular ions with gaseous molecules. V: theory
J. Chem. Phys., 1958, **29**, 294-299.

[58] N.G. Adams, D. Smith,
Ionic reactions in atmospheric, interstellar and laboratory plasmas,
Contemp. Phys., 1988, **29**, 559-578.

[59] R.A. Kennedy, C.A. Mayhew,
A study of the low energy electron attachment to trifluoromethyl sulphur pentafluoride, SF_5CF_3 : atmospheric implications,
Int. J. Mass Spectrom., 2001, **206**, i-iv.

[60] G.K. Jarvis, R.A. Kennedy, C.A. Mayhew,
Investigations of low energy electron attachment to SF_6, SeF_6 and TeF_6 using an electron swarm mass spectrometric technique
Int. J. Mass Spectrom., 2001, **205**, 253-270.

[61] A.A. Christodoulides, L.G. Christophorou, R.Y. Pai, C.M. Tung,
Electron attachment to perfluorocarbon compounds. I : *c*-C_4F_6, *2*-C_4F_6, *1,3*-C_4F_6, *c*-C_4F_8 and *2*-C_4F_8,
J. Chem. Phys., 1979, **70**, 1156-1168.

[62] C.A. Mayhew, A.D.J. Critchley, D.C. Howse, V.A. Mikhailov, M.A. Parkes,
Measurements of thermal electron attachment rate coefficients to molecules using an electron swarm technique.
Eur. Phys. J. D., 2005, **35**, 307-312.

[63] E.P. Grimsrud, S. Chowdbury, P. Kebarle,
The electron affinity of SF_6 and perfluoromethyl cyclohexane ; the unusual kinetics of electron transfer reactions $A^- + B \rightarrow A + B^-$,
J. Chem. Phys., 1985, **83**, 1059-1068.

[64] A. Hoxha, R. Locht, B. Leyh, D. Dehareng, K. Hottmann, H.W. Jochims, H. Baumgärtel,
Photoabsorption and constant ionic state spectroscopy of vinyl bromide,
Chem. Phys., 2000, **260**, 237-247.

[65] A.R. Ravishankara, S. Solomon, A.A. Turnipseed, R.F. Warren,
Atmospheric lifetimes of long-lived halogenated species,
Science, 1993, **259**, 194-199.

[66] T.N. Woods, W.K. Tobiska, G.J. Rottman, J.R. Worden,
Improved solar Lyman-α irradiance modelling from 1947-1999 based on UARS observations,
J. Geophys. Res. D., 2000, **105**, 27195-27215.

[67] H.J. Deyerl, L.S. Alconel, R.E. Continetti,
Photodetachment imaging studies of the electron affinity of CF_3,
J. Phys. Chem. A., 2001, **105**, 552-557.

[68] H.P. Fenzlaff, R. Gerhard, E. Illenberger,
Associative and dissociative electron attachment to SF_6 and SF_5Cl,
J. Chem. Phys., 1988**, 88**, 149-155.

[69] R. Schumacher, H.R. Sprunken, A.A. Christodoulides, R.N. Schindler,
Studies of electron cyclotron resonance technique ; electron scavenging properties of
CCl_3F, CCl_2F_2, $CClF_3$ and CF_4,
J. Phys. Chem., 1978, **82**, 2248-2252.

[70] J. Alvarez Ruiz, S. Ali, R.P. Tuckett,
Vacuum-UV fluorescence excitation spectroscopy of SF_5CF_3 in the range 8-25 eV,
unpublished data.

[71] H. Biehl, K.J. Boyle, R.P. Tuckett, H. Baumgärtel, H.W. Jochims,
Vacuum-UV fluorescence excitation spectroscopy of CF_3X (X = F,H,Cl,Br)
in the range 10-30 eV,
Chem. Phys., 1997, **214**, 367-382.

[72] A.R. Ravishankara, E.R. Lovejoy,
Atmospheric lifetime, and its application and determination : CFC-substitutes as a Case Study
J. Chem. Soc. Faraday Trans., 1994, **90**, 2159-2169.

[73] T. Gierczak, R.K. Talukdar, S.C. Herndon, G.L. Vaghjiani, A.R. Ravishankara,
Rate coefficients for the reaction of the OH radical with methane and substituted methanes,
J. Phys. Chem. A., 1997, **101**, 3125-3134.

[74] R.A. Morris, T.M. Miller, A.A. Viggiano, J.F. Paulson, S. Solomon, G. Reid,
Effects of electron and ion reactions on atmospheric lifetimes of fully fluorinated compounds,
J. Geophys. Res. D., 1995, **100**, 1287-1294.

[75] T. Reddmann, R. Ruhnke, W. Kouker,
Three-dimensional model simulations of SF_6 with mesospheric chemistry,
J. Geophys. Res. D., 2001, **106**, 14525-14537.

[76] T.M. Hall, D.W. Waugh,
Influence of nonlocal chemistry on tracer distributions : inferring the mean age of air from SF_6
J. Geophys. Res. D., 1998, **103**, 13327-13336.

[77] R.J. Cicerone,
Atmospheric carbon tetrafluoride : a nearly inert gas,
Science, 1979, **206**, 59-61.

Table Captions

Table 1 Examples of greenhouse gases, and their contribution to global warming [35-37].

Table 2 Appearance energies of fragment ions from SF_5CF_3 over the photoexcitation energy range 12.7-26.4 eV

Table 3 Total mean translational kinetic energy release, $\langle KE \rangle_T$, for the two-body fragmentation of the valence states of $SF_5CF_3^+$

Table 4 Rate coefficients, cation product ions and their branching ratios for the reactions of cations with possible atmospheric importance with SF_5CF_3. The recombination energies of the reagent cations are listed in eV in brackets under the cations. The capture rate coefficients, calculated using Langevin theory [57], are presented in square brackets under the experimental values. 0 K enthalpies of reaction for these channels are given in column 5. For formation of SF_3^+ and SF_4^+, two values for $\Delta_r H^o_0$ are given. The first value is calculated using the data set of Fisher *et al*. [43], whereas the second corresponds to that of Irikura [47]. The two values given for $\Delta_r H^o_0$ for formation of SF_5^+ by dissociative charge transfer result from taking the IE (SF_5) to be either 9.60 eV [43] or 9.71 eV [47].

Table 5 Possible products from e^- attachment and Lyman-α excitation of SF_5CF_3.

Table 6 Thermal electron attachment rate constants, absorption cross-sections at 121.6 nm, and atmospheric lifetimes for CF_4, SF_6 and SF_5CF_3.

Table 1. Examples of greenhouse gases, and their contribution to global warming [35-37].

Greenhouse Gas	**CO_2**	**CH_4**	**N_2O**	**CF_2Cl_2**	**SF_5CF_3**
Concentration in 1998 / ppmv	365	1.75	0.31	0.0005	1.2×10^{-7}
ΔConcentration (1750–1998) / ppmv	87	1.045	0.044	0.0005	1.2×10^{-7}
ΔConcentration (*ca.* 2000) / % pa	0.45	0.60	0.25	*ca.* 5.0	*ca.* 6.3
Radiative forcing a_o / W m^{-2} $ppbv^{-1}$	1.68×10^{-5}	4.59×10^{-4}	3.41×10^{-3}	0.32	0.60
Total radiative forcing [a] / W m^{-2}	1.46	0.48	0.15	0.16	7.2×10^{-5}
Lifetime [b] / years	50-200 [c]	12	120	102	*ca.* 1000
Global warming potential [d]	1	23	296	10600	> 17500
Contribution to greenhouse effect / %	52	17	5	*ca.* 15 [e]	<< 0.01

[a] Due to change in concentration of greenhouse gas from the pre-Industrial era to the present time.
[b] Assumes a single-exponential decay for removal of greenhouse gas from the atmosphere.
[c] CO_2 does not show a single-exponential decay [37,38].
[d] Calculated for a time period of 100 years.
[e] Cumulative effect of all chlorofluorocarbons.

Table 2 Appearance energies of fragment ions from SF_5CF_3 over the photoexcitation energy range 12.7-26.4 eV

Fragment ion	AE_{298} / eV	Neutral partner	$\Delta_r H^o_0$ / eV
Major ions [a]			
CF_3^+	12.92 ± 0.18	SF_5	12.90
SF_5^+	13.9 ± 1.2	CF_3	13.67
Minor ions [b]			
SF_4^+	13.5 ± 1.3	CF_4	12.42
SF_3^+	14.94 ± 0.13	CF_4 + F	12.36
CF_2^+	16.0 ± 2.0	SF_6	15.22

[a] A *major* ion is defined as one formed by a single bond cleavage ; formation of CF_3^+ and SF_5^+ involves cleavage of the S-C bond.

[b] A *minor* ion is defined as one in which intramolecular rearrangement must occur. Note that the formation of SF_4^+, SF_3^+ and CF_2^+ is only possible at their observed appearance energies given in Column 2 if migration of F^- across the S–C bond occurs in the transition state to form CF_4 and SF_6, respectively, as accompanying neutrals.

Table 3 Total mean translational kinetic energy release, $\langle KE \rangle_T$, for the two-body fragmentation of the valence states of $SF_5CF_3^+$

Fragment	E / eV	E_{avail} / eV [a]	$\langle KE \rangle_T$ / eV	f_{expt}	$f_{statistical}$ [b]	$f_{pure\ impulsive}$ [c]
CF_3^+ [d]	14.25	1.52	0.32 (5)	0.21	0.04	0.20
	15.69	2.96	0.29 (2)	0.10	0.04	0.20
	16.98	4.25	0.38 (1)	0.09	0.04	0.20
	17.97	5.24	0.40 (1)	0.08	0.04	0.20
	19.07	6.34	0.37 (1)	0.06	0.04	0.20

[a] E_{avail} is defined in equ. (VII). The average thermal energy of SF_5CF_3 is 0.17 eV.
[b] From Klots [50].
[c] From Holdy, Klotz and Wilson [42].
[d] Assumes the neutral fragment is SF_5.

Table 4 Rate coefficients, cation product ions and their branching ratios for the reactions of cations with possible atmospheric importance with SF_5CF_3. The recombination energies of the reagent cations are listed in eV in brackets under the cations. The capture rate coefficients, calculated using Langevin theory [57], are presented in square brackets under the experimental values. 0 K enthalpies of reaction for these channels are given in column 5. For formation of SF_3^+ and SF_4^+, two values for $\Delta_r H^o_0$ are given. The first value is calculated using the data set of Fisher *et al*. [43], whereas the second corresponds to that of Irikura [47]. The two values given for $\Delta_r H^o_0$ for formation of SF_5^+ by dissociative charge transfer result from taking the IE (SF_5) to be either 9.60 eV [43] or 9.71 eV [47].

Reagent Ion	Rate Coefficient / x 10^{-9} cm^3 s^{-1}	Product Ion / %	Proposed Neutral Products	$\Delta_r H^o_0$ / kJ mol^{-1}
N_2^+	1.6	CF_3^+ (65)	$SF_5 + N_2$	-258
(15.58)	[1.4]	SF_3^+ (28)	$CF_4 + F + N_2$	-248, -289
		SF_4^+ (trace)	$CF_4 + N_2$	-283, -345
		$SF_4^+CF_3$ (2)	$F + N_2$	?
		SF_5^+ (5)	$CF_3 + N_2$	-185, -175
N^+	2.2	CF_3^+ (80)	$SF_5 + N$	-157
(14.53)	[1.9]	SF_3^+ (17)	$CF_4 + F + N$	-147, -187
		SF_4^+ (trace)	$CF_4 + N$	-181, -243
		SF_5^+ (3)	$CF_3 + N$	-84, -73
CO^+	1.6	CF_3^+ (75)	$SF_5 + CO$	-107
(14.01)	[1.4]	SF_3^+ (22)	$CF_4 + F + CO$	-96, -137
		SF_4^+ (trace)	$CF_4 + CO$	-131, -193
		SF_5^+ (3)	$CF_3 + CO$	-34 (± 43), -23 (± 46)
CO_2^+	1.2	CF_3^+ (76)	$SF_5 + CO_2$	-84
(13.77)	[1.1]	SF_3^+ (14)	$CF_4 + F + CO_2$	-73, -114
		SF_4^+ (8)	$CF_4 + CO_2$	-108, -170
		SF_5^+ (2)	$CF_3 + CO_2$	-11 (± 43), 0 (± 46)
O^+	1.9	CF_3^+ (83)	$SF_5 + O$	-69
(13.62)	[1.8]	SF_3^+ (16)	$CF_4 + F + O$	-59, -100
		SF_4^+ (trace)	$CF_4 + O$	-93, -156
		SF_5^+ (1)	$CF_3 + O$	4 (± 43), 14 (± 46)
N_2O^+	1.1	CF_3^+ (75)	$SF_5 + N_2O$	1 (± 39)
(12.89)	[1.1]	SF_3^+ (19)	$CF_4 + F + N_2O$	12 (± 45), -29 (± 47)
		SF_4^+ (5)	$CF_4 + N_2O$	-23 (± 45), -85
		SF_5^+ (1)	$CF_3 + N_2O$	74, 84
H_2O^+	1.6	CF_3^+ (8)	$SF_5 + H_2O$	28 (± 39)
(12.61)	[1.7]	SF_3^+ (92)	$CF_4 + F + H_2O$	39 (± 45), -2 (± 47)
		SF_4^+ (trace)	$CF_4 + H_2O$	4 (± 45), -58
O_2^+	0.01	CF_3^+ (63)	$SF_5 + O_2$	80, 62, 43 (±39) [a]
(12.07)	[1.3]	SF_3^+ (31)	$CF_4 + F + O_2$	91, 50 (± 47)
		SF_4^+ (2)	$CF_4 + O_2$	56, -6 (± 46)
		SF_5^+ (4)	$CF_3 + O_2$	153, 164

[a] The three values given are for the $v = 0$, 1 and 2 vibrational levels of O_2^+, respectively.

Table 5 Possible products from e^- attachment and Lyman-α excitation of SF_5CF_3

Reaction		$\Delta_r H^o_0$ / kJ mol-1 (eV) Scheme A [a]	Scheme B [b]
$SF_5CF_3 + e^-$ (0 eV) (–1623 or –1750)	→ SF_5^- (–1282) [c] + CF_3 (–463) [c]	–122 (–1.26)	+5 (+0.05)
	→ CF_3^- (–639) + SF_5 (–915)	+69 (+0.72)	+196 (+2.03)
SF_5CF_3 + hν (10.2 eV) (-1623 or -1750)	→ SF_5 (–915) + CF_3 (–463)	–739 (–7.66)	–612 (–6.34)
	→ CF_3^+ (+409) + SF_5^- (–1282)	–234 (–2.43)	–107 (–1.11)
	→ SF_5^+ (+29) + CF_3^- (–639)	+29 (+0.30)	+156 (+1.62)

[a] Scheme A assumes $\Delta_f Ho_0$ (SF_5CF_3) = –1623 kJ mol-1 (theory [32]).

[b] Scheme B assumes $\Delta_f Ho_0$ (SF_5CF_3) = –1750 kJ mol-1 (experiment : updated value from [20]).

[c] Values in brackets are $\Delta_f Ho_0$ in kJ mol^{-1}.

Table 6 Thermal electron attachment rate constants, absorption cross-sections at 121.6 nm, and atmospheric lifetimes for CF_4, SF_6 and SF_5CF_3.

Perfluoro compound	k_e (298 *K*) / $cm^3\ s^{-1}$	$\sigma_{121.6}$ / cm^2	lifetime / years
CF_4	$< 10^{-16}$ [a]	$< 8 \times 10^{-22}$ [b]	> 50000
SF_6	2.38×10^{-7} [c]	1.76×10^{-18} [b]	> 800
SF_5CF_3	7.7×10^{-8} [d]	1.3×10^{-17} [e]	*ca.* 1000

[a] Schumacher *et al.* [69].
[b] Ravishankara *et al.* [65].
[c] Mayhew *et al.* [62].
[d] Kennedy and Mayhew [59].
[e] Re-analysis of the data of Chim *et al.* [16], resulting in a reduction of $\sigma_{121.6}$ by 2 Mb.

Figure captions

Figure 1 : Electron density map of the highest occupied molecular orbital of $SF_5–CF_3$. The FSF and FCF bond angles are all either 90^o or 109.3^o. The S–C bond length is 0.186 nm, the three C–F lengths all 0.130 nm, the three $S–F_{equitorial}$ lengths are 0.158 nm, and the two $S–F_{axial}$ lengths are 0.157 nm. The dipole moment is calculated to be 0.95 Debye.

Figure 2 Definition of the dissociative ionisation energy (DIE) of a generalised polyatomic molecule AB–CD. In the particular application to SF_5CF_3, AB represents CF_3, CD represents SF_5.

Figure 3 Extrapolation method to determine the first dissociative ionisation energy of AB–CD.

Figure 4 Schematic of the threshold photoelectron photoion coincidence apparatus. The apparatus can also study coincidences between threshold photoelectrons or mass-resolved cations with fluorescence photons, but these modes of operation are not used in this work.

Figure 5 Results of the extrapolation experiment for $CF_3^+ + SF_5$ from SF_5CF_3. Only datapoints that define the Franck-Condon region of the ground state of $SF_5CF_3^+$ are used to define the slope and intercept of the graph [17]. The slope is 0.19, and the first dissociative ionisation energy of SF_5CF_3 is determined to be 12.9 ± 0.4 eV. (Reproduced by permission from *J. Phys. Chem. A.,* 2001, **105**, 8403-8412.)

Figure 6 TPEPICO-TOF spectrum (closed circles) for CF_3^+ / SF_5CF_3 recorded at a photon energy of 14.09 eV. Shown as a solid line, the data fit to a mean translational KE release, $<KE>_T$, of 0.24 ± 0.05 eV. (Reproduced by permission from *J. Phys. Chem. A.,* 2001, **105**, 8403-8412.)

Figure 7 Threshold photoelectron spectrum of SF_5CF_3 recorded at a resolution of 0.3 nm. Assignment of the bands to the ground state ($\widetilde{X}$) and excited electronic states ($\widetilde{A}$, $\widetilde{B}$, $\widetilde{C}$, *etc.*) of $SF_5CF_3^+$ is shown. (Reproduced by permission from *J. Phys. Chem. A.,* 2001, **105**, 8403-8412.)

Figure 8 Time-of-flight spectrum of fragmant ions from SF_5CF_3 integrated over the photoexcitation energies 12.7-26.4 eV. (Reproduced by permission from *J. Phys. Chem. A.,* 2001, **105**, 8403-8412.)

Figure 9 Schematic of the selected ion flow tube used to determine rate coefficients and product ion yields of ion-molecule reactions. (Reproduced by permision of Dr C R Howle, PhD thesis, University of Birmingham, 2004.)

Figure 10 Schematic of the electron swarm drift tube used in Birmingham for the SF_5CF_3 measurements. A small pinhole at the right-hand end of the drift tube leads *via* differential pumping, to a quadrupole mass spectrometer for detection of the anionic products. (Reproduced by permission from *Int. J. Mass Spectrom.,* 2001, **205**, 253-270.)

Figure 11 Graph of electron attachment rate coefficient, k_a, as a function of mean electron energy for SF_5CF_3 in atmospheric pressure of N_2 ($<\varepsilon>$ less than 0.5 eV) and Ar ($<\varepsilon>$ greater than 0.5 eV) buffer gas. (Reproduced by permission from *Int. J. Mass Spectrom.,* 2001, **206**, i-iv.)

Figure 12 Apparatus used to record the vacuum-UV absorption spectrum of SF_5CF_3. (Reproduced by permission from *Chem. Phys.,* 2000, **260**, 237-247.)

Figure 13 Absorption spectrum of SF_5CF_3 recorded with a photon resolution of 0.08 nm. The absorption cross section at 121.6 nm is $1.3 \pm 0.2 \times 10^{-17}$ cm^2 *or* 13 ± 2 Mb. (Reproduced by permission from *Chem. Phys. Letts.,* 2003, **367**, 697-703.)

Figure 1 : Electron density map of the highest occupied molecular orbital of $SF_5–CF_3$. The FSF and FCF bond angles are all either 90^o or 109.3^o. The S–C bond length is 0.186 nm, the three C–F lengths all 0.130 nm, the three $S–F_{equitorial}$ lengths are 0.158 nm, and the two $S–F_{axial}$ lengths are 0.157 nm. The dipole moment is calculated to be 0.95 Debye.

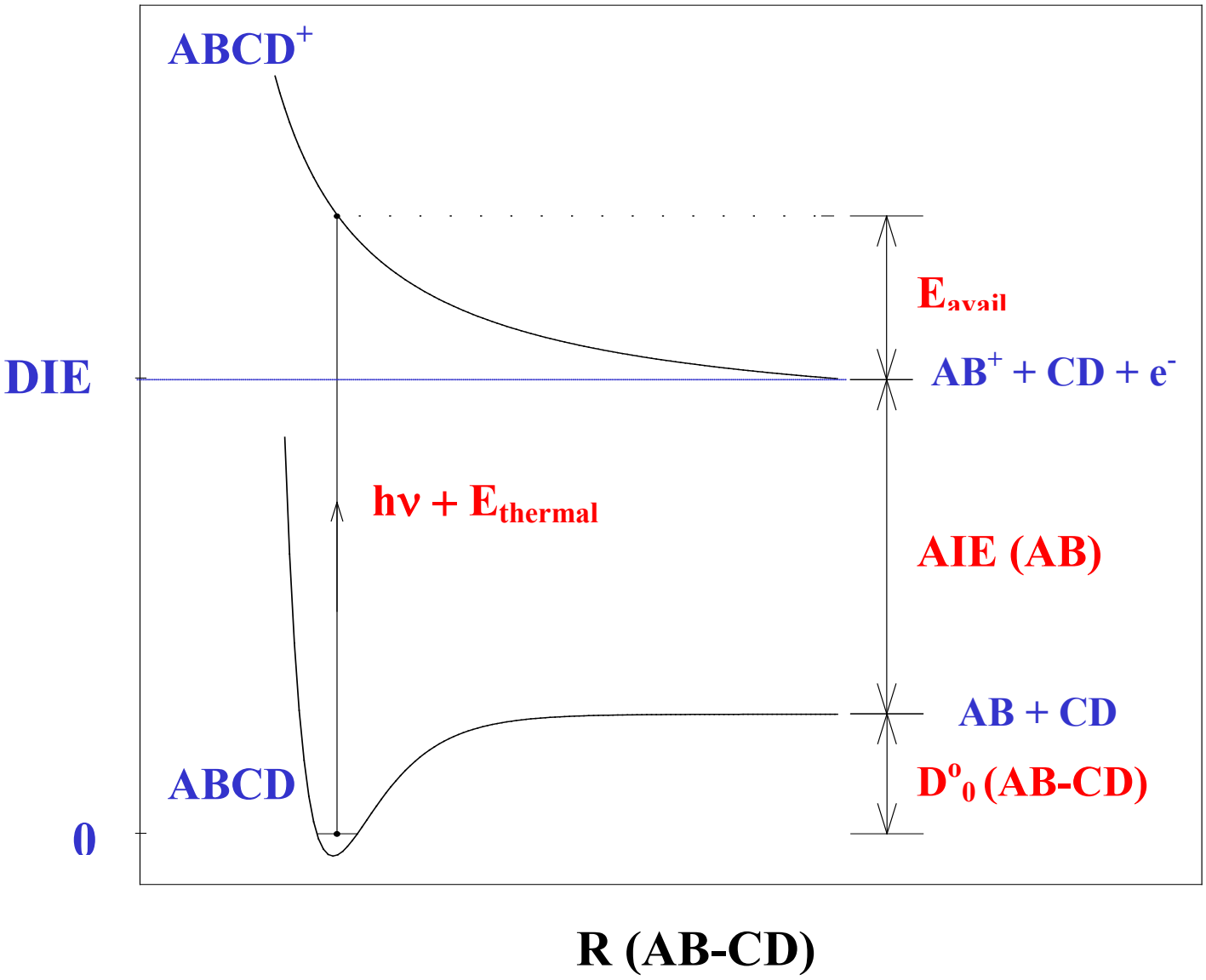

Figure 2 Definition of the dissociative ionisation energy (DIE) of a generalised polyatomic molecule AB–CD. In the particular application to SF_5CF_3, AB represents CF_3, CD represents SF_5.

+

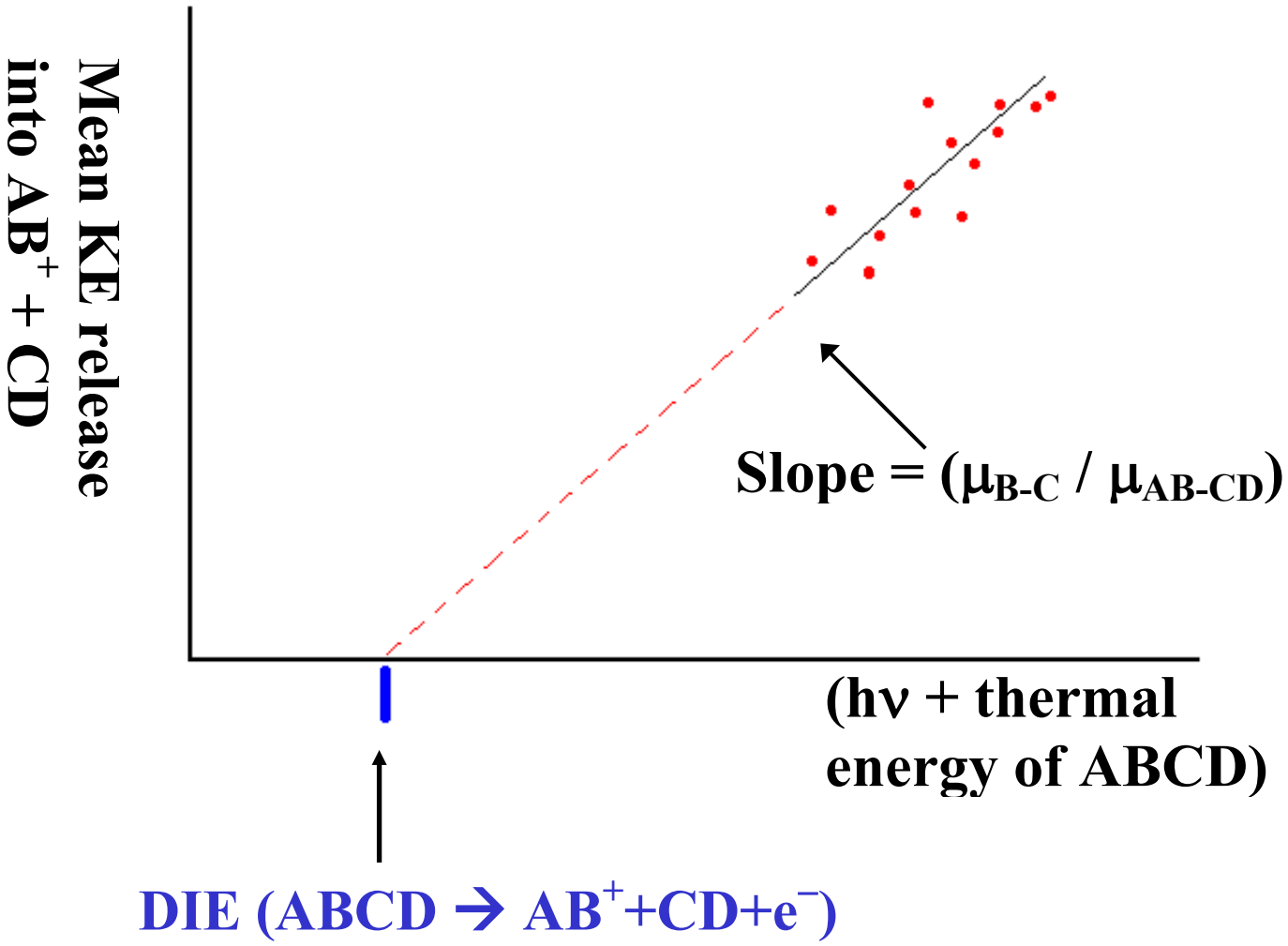

Figure 3 Extrapolation method to determine the first dissociative ionisation energy of AB–CD.

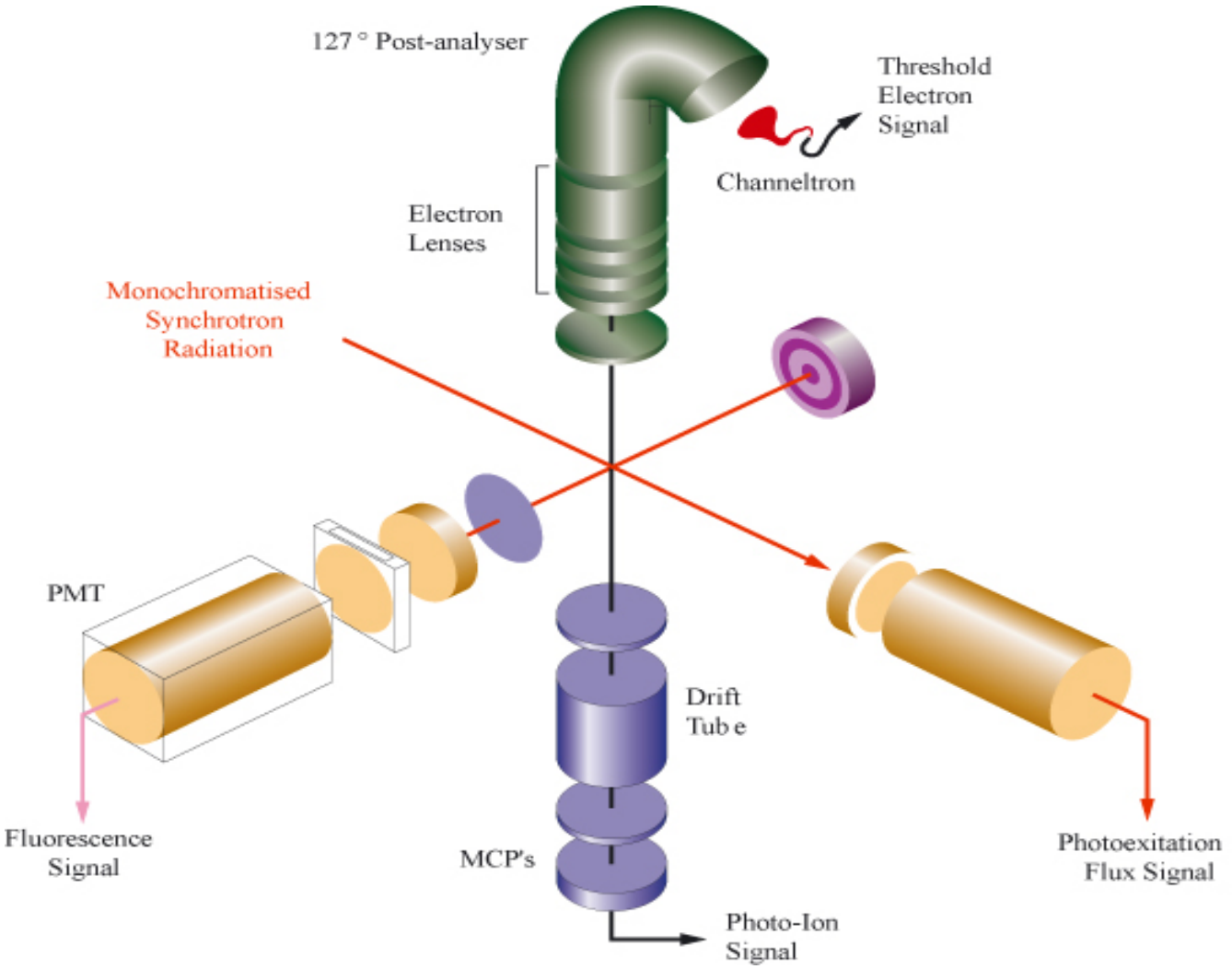

Figure 4 Schematic of the threshold photoelectron photoion coincidence apparatus. The apparatus can also study coincidences between threshold photoelectrons or mass-resolved cations with fluorescence photons, but these modes of operation are not used in this work.

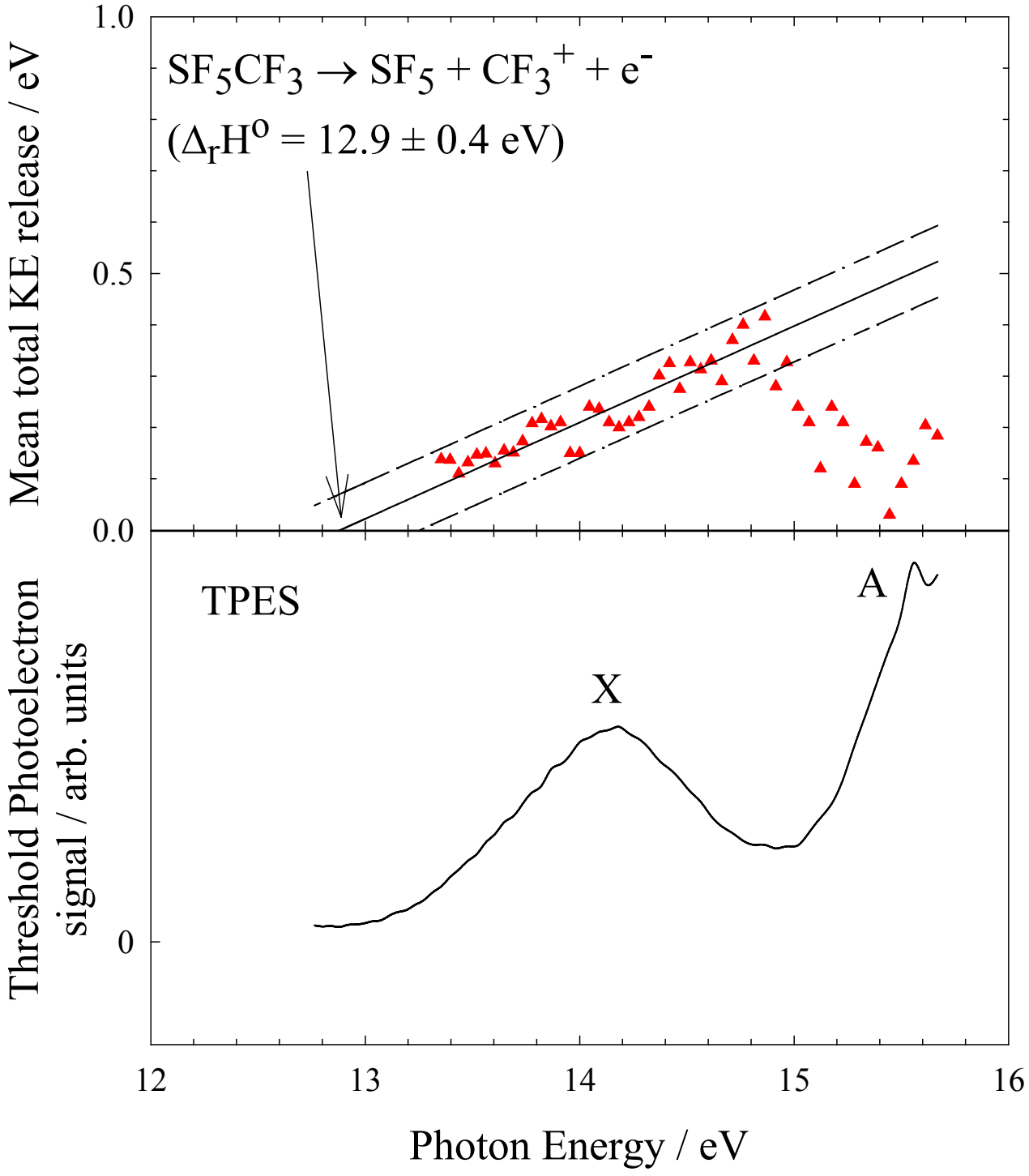

Figure 5 Results of the extrapolation experiment for $CF_3^+ + SF_5$ from SF_5CF_3. Only datapoints that define the Franck-Condon region of the ground state of $SF_5CF_3^+$ are used to define the slope and intercept of the graph [17]. The slope is 0.19, and the first dissociative ionisation energy of SF_5CF_3 is determined to be 12.9 ± 0.4 eV. (Reproduced by permission from *J. Phys. Chem. A.,* 2001, **105**, 8403-8412.)

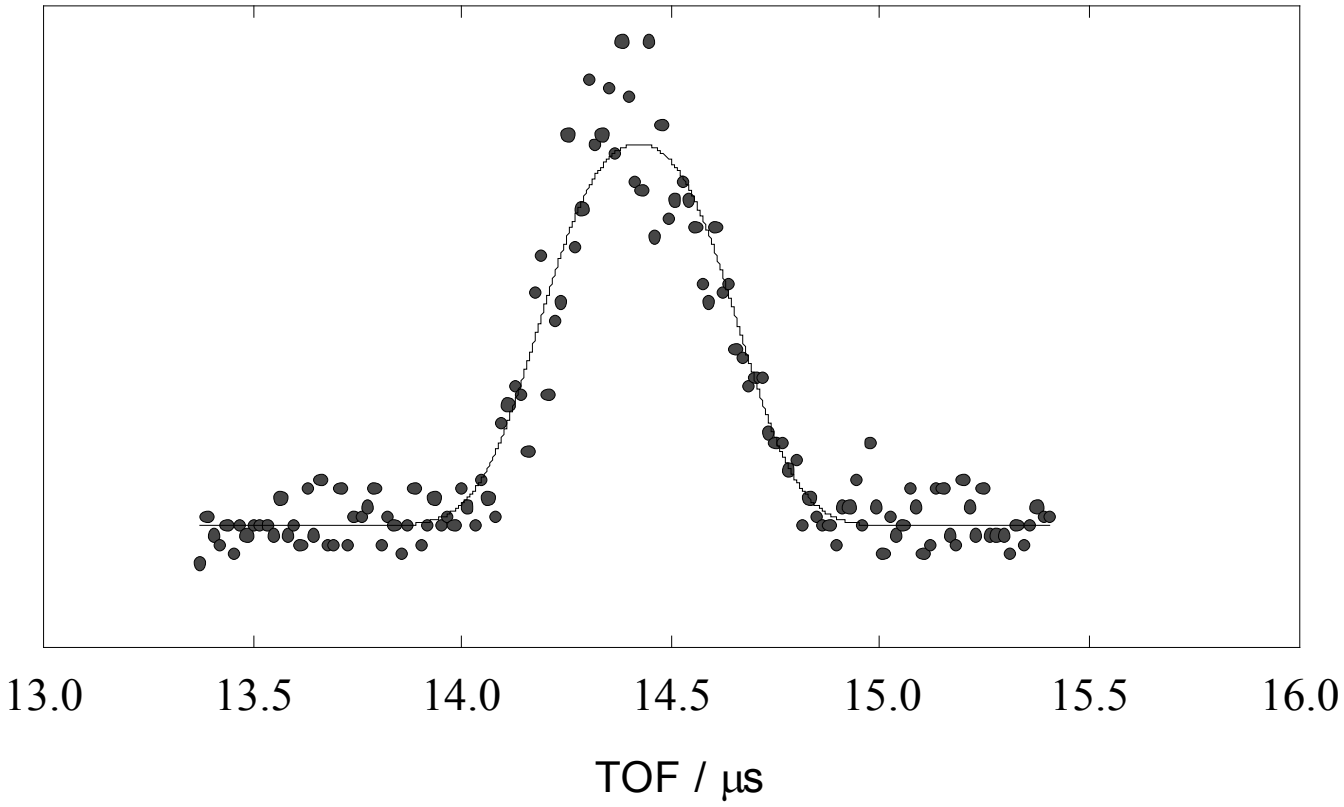

Figure 6 TPEPICO-TOF spectrum (closed circles) for CF_3^+ / SF_5CF_3 recorded at a photon energy of 14.09 eV. Shown as a solid line, the data fit to a mean translational KE release, $\langle KE \rangle_T$, of 0.24 ± 0.05 eV. (Reproduced by permission from *J. Phys. Chem. A.,* 2001, **105**, 8403-8412.)

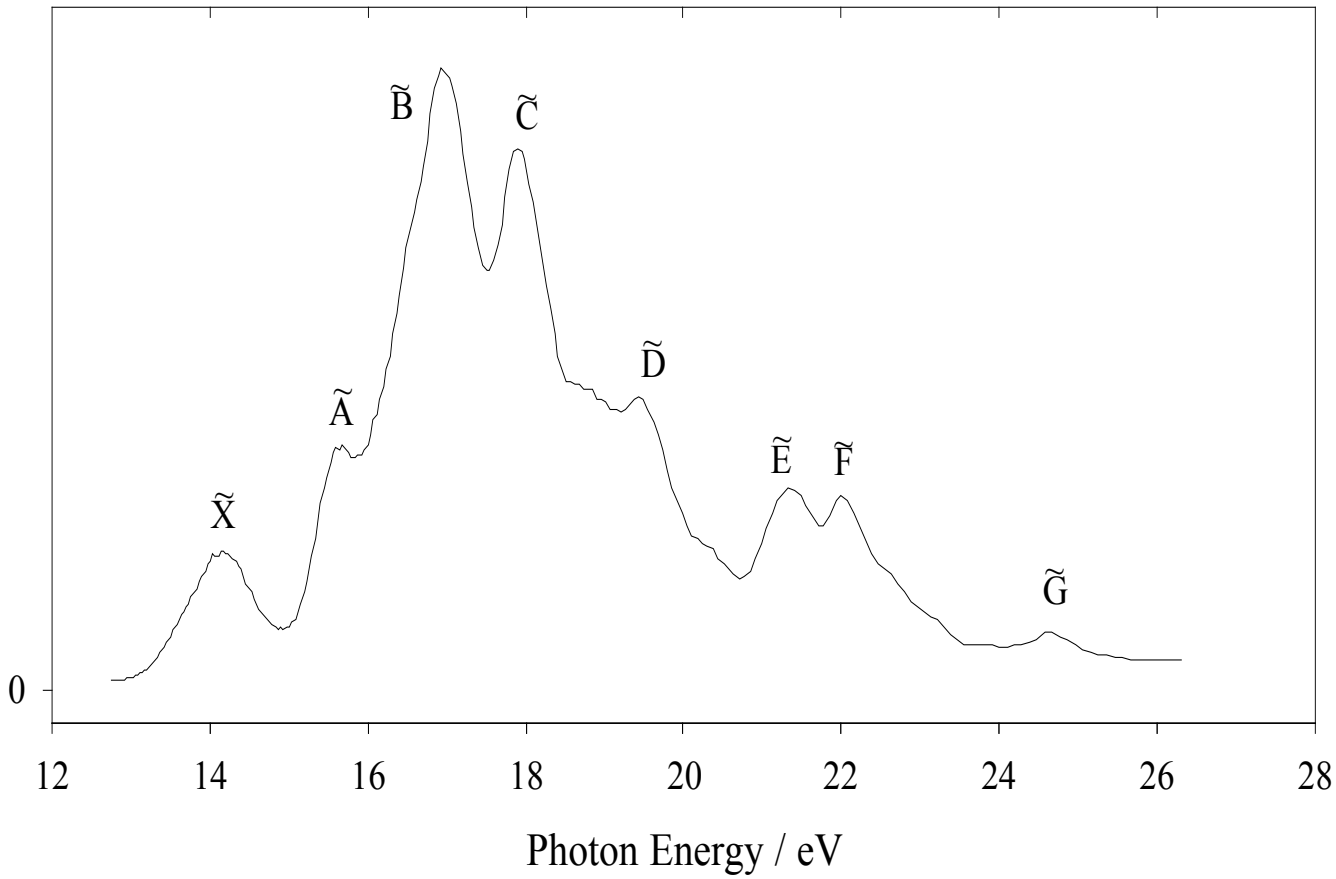

Figure 7 Threshold photoelectron spectrum of SF_5CF_3 recorded at a resolution of 0.3 nm. Assignment of the bands to the ground state ($\tilde{X}$) and excited electronic states ($\tilde{A}$, $\tilde{B}$, $\tilde{C}$, *etc.*) of $SF_5CF_3^+$ is shown. (Reproduced by permission from *J. Phys. Chem. A.,* 2001, **105**, 8403-8412.)

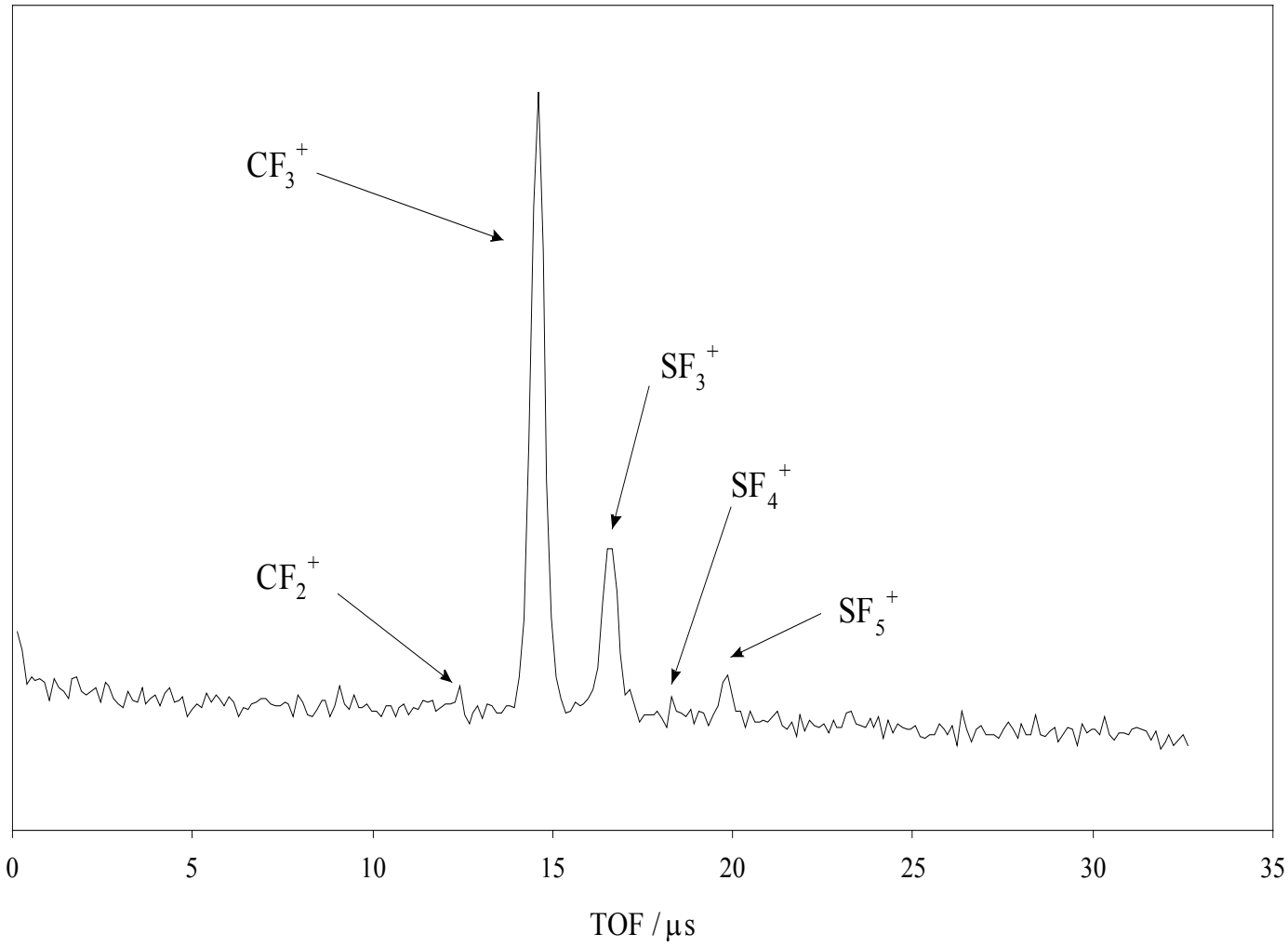

Figure 8 Time-of-flight spectrum of fragmant ions from SF_5CF_3 integrated over the photoexcitation energies 12.7-26.4 eV. (Reproduced by permission from *J. Phys. Chem. A.,* 2001, **105**, 8403-8412.)

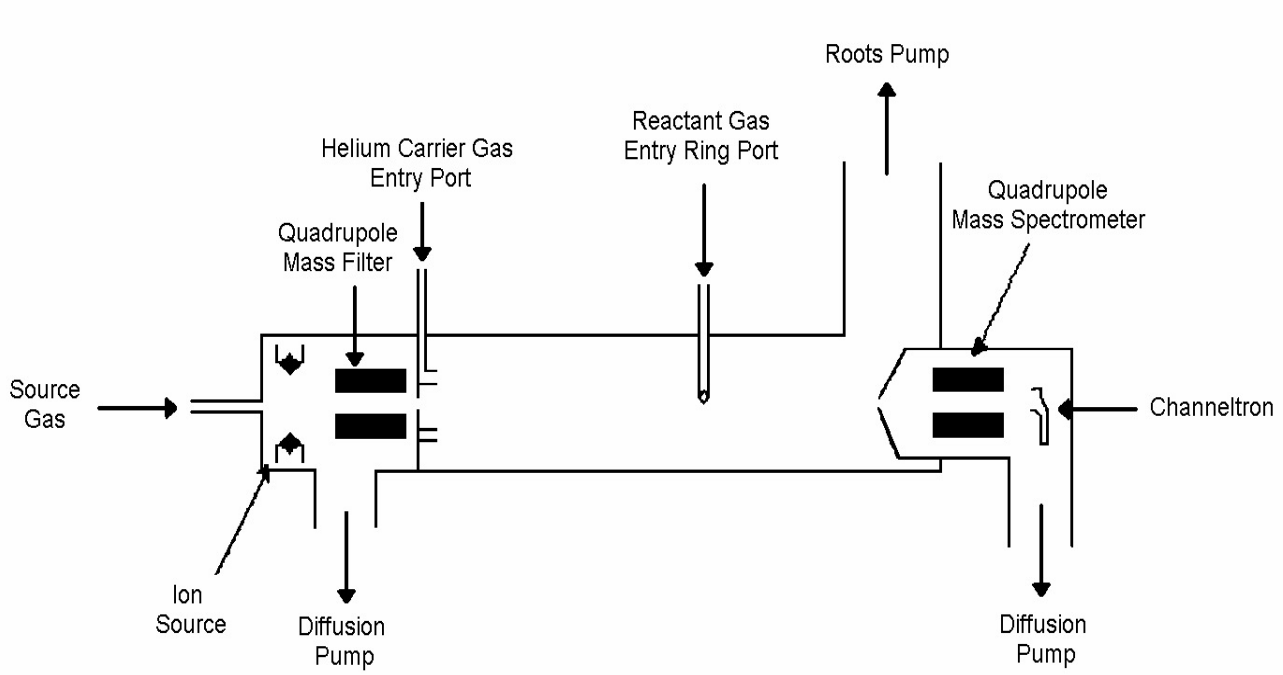

Figure 9 Schematic of the selected ion flow tube used to determine rate coefficients and product ion yields of ion-molecule reactions. (Reproduced by permision of Dr C R Howle, PhD thesis, University of Birmingham, 2004.)

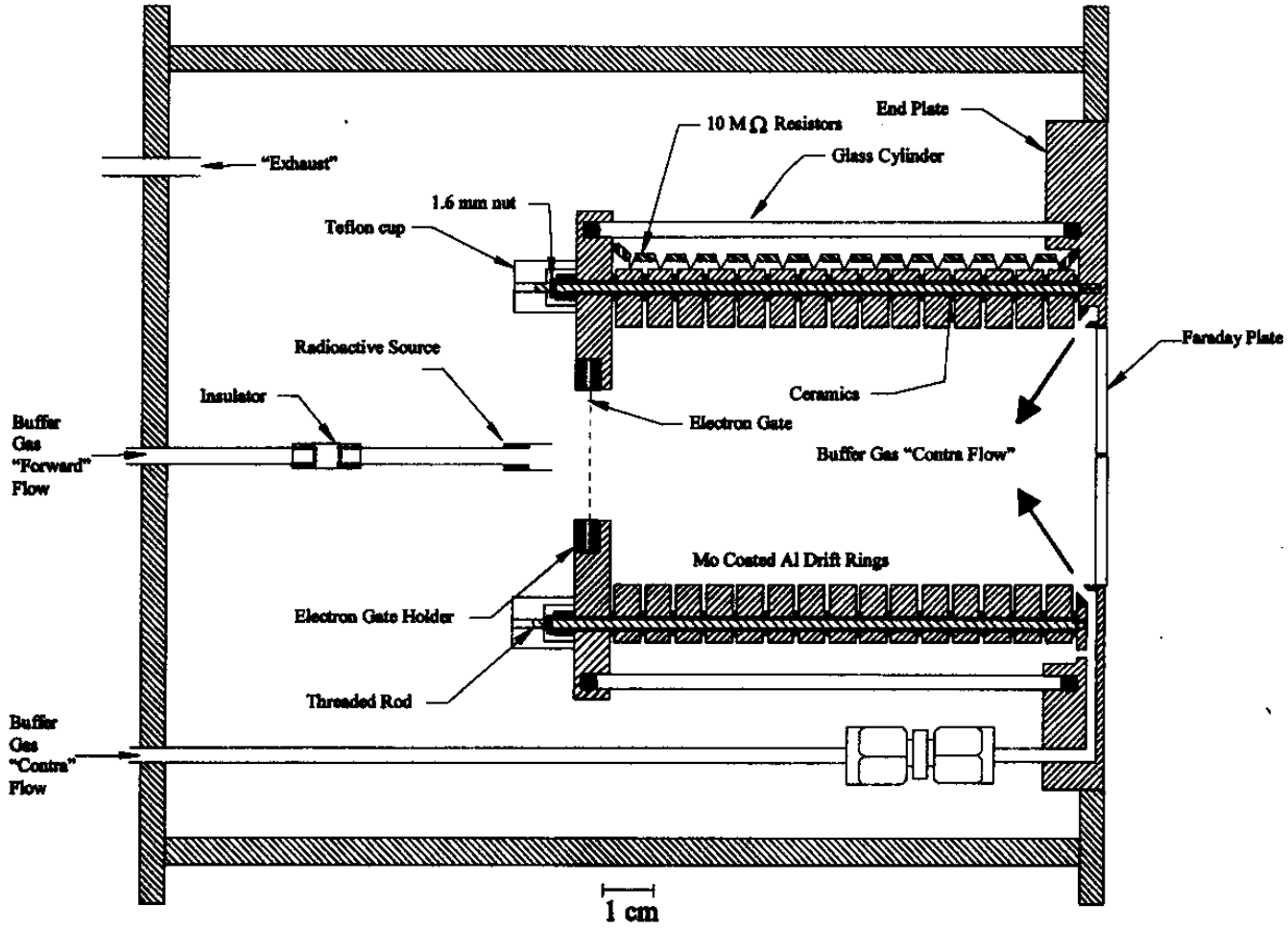

Figure 10 Schematic of the electron swarm drift tube used in Birmingham for the SF_5CF_3 measurements. A small pinhole at the right-hand end of the drift tube leads *via* differential pumping, to a quadrupole mass spectrometer for detection of the anionic products. (Reproduced by permission from *Int. J. Mass Spectrom.,* 2001, **205**, 253-270.)

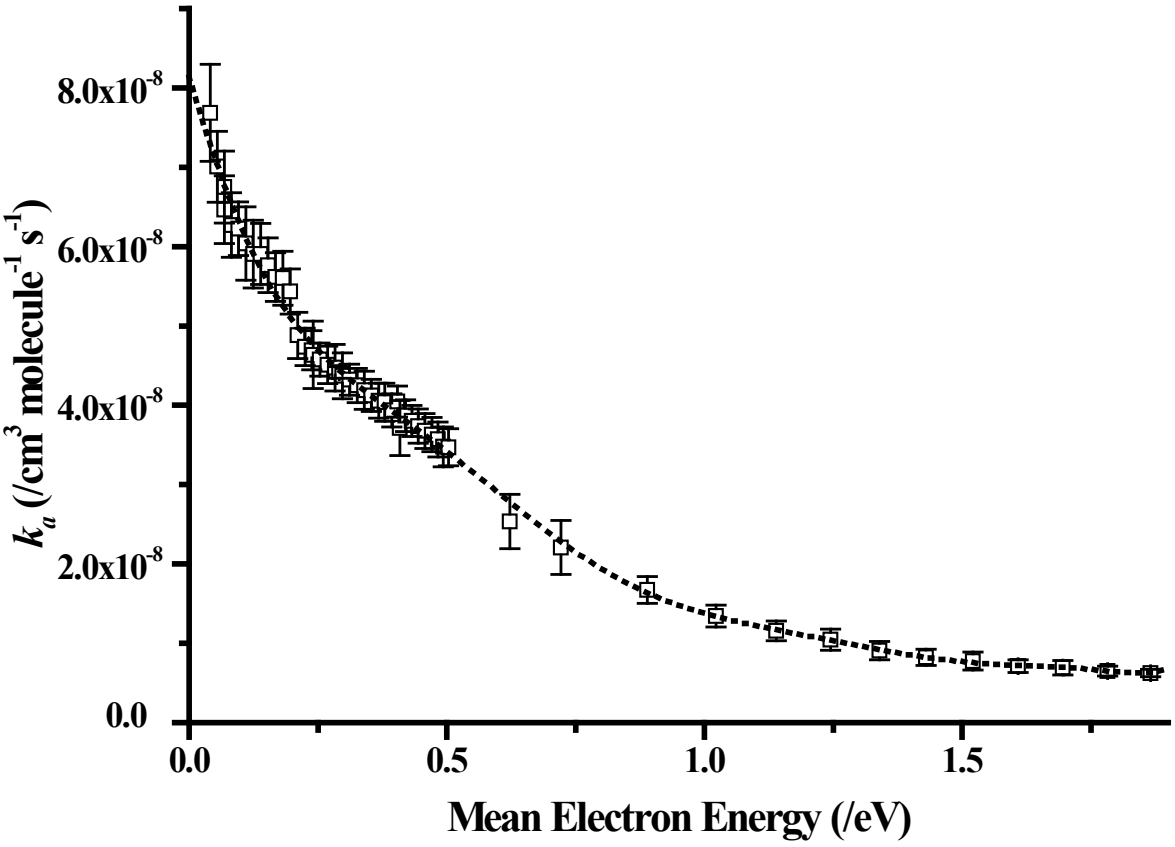

Figure 11 Graph of electron attachment rate coefficient, k_a, as a function of mean electron energy for SF_5CF_3 in atmospheric pressure of N_2 (<ε> less than 0.5 eV) and Ar (<ε> greater than 0.5 eV) buffer gas. (Reproduced by permission from *Int. J. Mass Spectrom.,* 2001, **206**, i-iv.)

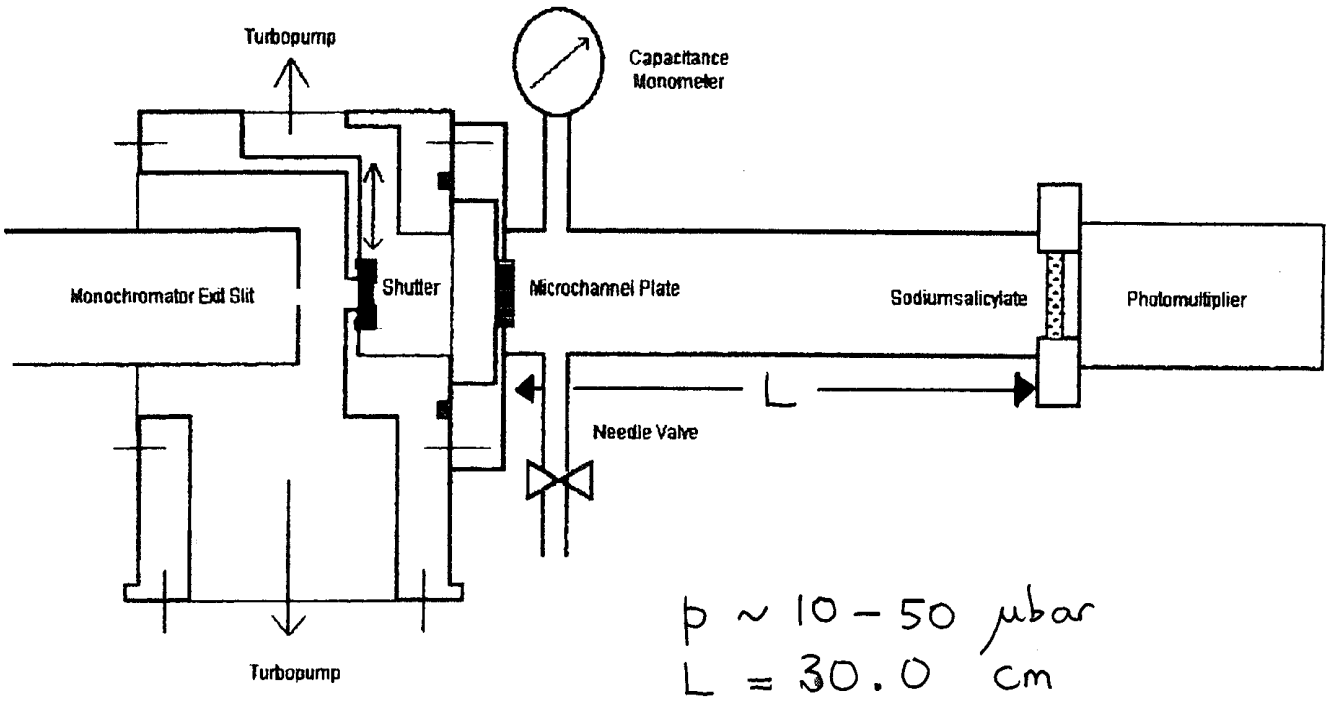

Figure 12 Apparatus used to record the vacuum-UV absorption spectrum of SF_5CF_3. (Reproduced by permission from *Chem. Phys.,* 2000, **260**, 237-247.)

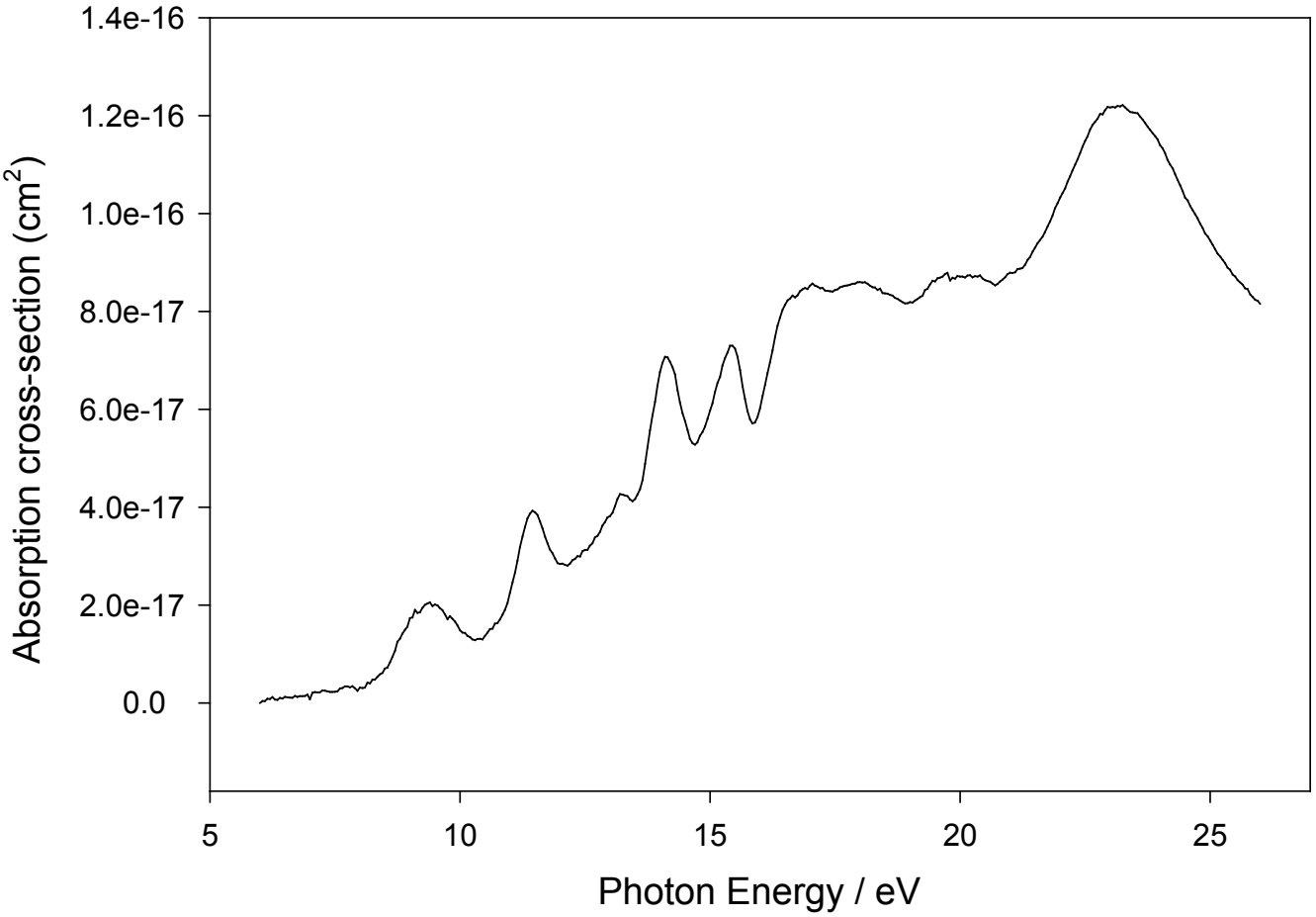

Figure 13 Absorption spectrum of SF_5CF_3 recorded with a photon resolution of 0.08 nm. The absorption cross section at 121.6 nm is $1.3 \pm 0.2 \times 10^{-17}$ cm^2 *or* 13 ± 2 Mb. (Reproduced by permission from *Chem. Phys. Letts.,* 2003, **367**, 697-703.)